Epidemics xxx (2017) xxx–xxx

Contents lists available at ScienceDirect

Epidemics

journal homepage: www.elsevier.com/locate/epidemics

Modelling H5N1 in Bangladesh across spatial scales: Model complexity and zoonotic transmission risk

Edward M. Hill[a,b,*], Thomas House[c], Madhur S. Dhingra[d,e], Wantanee Kalpravidh[f], Subhash Morzaria[g], Muzaffar G. Osmani[h], Mat Yamage[i,1], Xiangming Xiao[j], Marius Gilbert[d,k], Michael J. Tildesley[b,l,m]

[a] Centre for Complexity Science, University of Warwick, Coventry, CV4 7AL, United Kingdom
[b] Zeeman Institute: Systems Biology and Infectious Disease Epidemiology Research (SBIDER), University of Warwick, Coventry, CV4 7AL, United Kingdom
[c] School of Mathematics, The University of Manchester, Manchester, M13 9PL, United Kingdom
[d] Spatial Epidemiology Lab (SpELL), Université Libre de Bruxelles, B-1050 Brussels, Belgium
[e] Department of Animal Husbandry and Dairying, Government of Haryana, Panchkula, India
[f] Food and Agricultural Organization of the United Nations Regional Office for Asia and the Pacific, Bangkok, Thailand
[g] Food and Agricultural Organization of the United Nations, Rome, Italy
[h] Department of Livestock Services, Dhaka, Bangladesh
[i] Emergency Centre for Transboundary Animal Diseases (ECTAD), Food and Agriculture Organization of the United Nations, Dhaka, Bangladesh
[j] Department of Microbiology and Plant Biology, Center for Spatial Analysis, University of Oklahoma, Norman, OK 73019, United States
[k] Fonds National de la Recherche Scientifique, B-1000 Brussels, Belgium
[l] School of Life Sciences, University of Warwick, Coventry, CV4 7AL, United Kingdom
[m] Mathematics Institute, University of Warwick, Coventry, CV4 7AL, United Kingdom

ARTICLE INFO

Article history:
Received 2 September 2016
Received in revised form 15 February 2017
Accepted 17 February 2017
Available online xxx

Keywords:
Influenza A
H5N1
Mathematical modelling
Epidemiology

ABSTRACT

Highly pathogenic avian influenza H5N1 remains a persistent public health threat, capable of causing infection in humans with a high mortality rate while simultaneously negatively impacting the livestock industry. A central question is to determine regions that are likely sources of newly emerging influenza strains with pandemic causing potential. A suitable candidate is Bangladesh, being one of the most densely populated countries in the world and having an intensifying farming system. It is therefore vital to establish the key factors, specific to Bangladesh, that enable both continued transmission within poultry and spillover across the human–animal interface. We apply a modelling framework to H5N1 epidemics in the Dhaka region of Bangladesh, occurring from 2007 onwards, that resulted in large outbreaks in the poultry sector and a limited number of confirmed human cases. This model consisted of separate poultry transmission and zoonotic transmission components. Utilising poultry farm spatial and population information a set of competing nested models of varying complexity were fitted to the observed case data, with parameter inference carried out using Bayesian methodology and goodness-of-fit verified by stochastic simulations. For the poultry transmission component, successfully identifying a model of minimal complexity, which enabled the accurate prediction of the size and spatial distribution of cases in H5N1 outbreaks, was found to be dependent on the administration level being analysed. A consistent outcome of non-optimal reporting of infected premises materialised in each poultry epidemic of interest, though across the outbreaks analysed there were substantial differences in the estimated transmission parameters. The zoonotic transmission component found the main contributor to spillover transmission of H5N1 in Bangladesh was found to differ from one poultry epidemic to another. We conclude by discussing possible explanations for these discrepancies in transmission behaviour between epidemics, such as changes in surveillance sensitivity and biosecurity practices.

* Corresponding author at: Centre for Complexity Science, University of Warwick, Coventry, CV4 7AL, United Kingdom
E-mail address: Edward.Hill@warwick.ac.uk (E.M. Hill).
[1] Current address: Sengen, Tsukuba, Ibaraki 305-0047, Japan.

http://dx.doi.org/10.1016/j.epidem.2017.02.007
1755-4365/

1. Introduction

The H5N1 subtype of highly pathogenic avian influenza (HPAI) has caused considerable concern since the initial observation of the virus in southern China during 1996 (Sims et al., 2005). From the time of the first large-scale epizootic that took place in the winter of 2003/2004 in East and Southeast Asia (Alexander, 2007), H5N1 has killed or forced the culling of more than 400 million domestic poultry and resulted in an estimated US$20 billion in economic damage, with 63 countries infected at its peak in 2006 (FAO-DAH, 2012). Being a zoonotic disease H5N1 HPAI remains a persistent public health threat, capable of causing infection in humans with a high mortality rate. Since 2003 it has caused over 850 laboratory-confirmed human cases across 16 countries, leading to subsequent deaths in 14 of these nations, with the cumulative death total exceeding 450 (World Health Organisation, 2016).

With a number of countries in South and Southeast Asia, including China, Vietnam, Indonesia and Bangladesh, being gravely affected, a number of studies have predominately focused on either spatio-temporal analysis of outbreaks (Pfeiffer et al., 2007; Ahmed et al., 2010, 2011; Minh et al., 2011; Dhingra et al., 2014), or on determining ecological/environmental risk factors for H5N1 avian influenza emergence and spread at region-wide (Gilbert et al., 2008), national (Gilbert et al., 2007; Van Boeckel et al., 2012; Loth et al., 2010) and sub-national levels (Henning et al., 2009). For example, H5N1 poultry epidemics in Thailand have been associated with the following risk factors: rice crop intensity, free grazing ducks and water presence (Gilbert et al., 2007; Van Boeckel et al., 2012). Across studies and regions three types of variables with similar statistical association with H5N1 were identified: domestic waterfowl, human related variables (e.g. human population density) and indicators of water presence (Gilbert and Pfeiffer, 2012).

Bangladesh is one of the most densely populated countries in the world, with a human population exceeding 160 million (United Nations, 2015). In combination with an intensifying farming system and substantial poultry population (1194 birds/km^2) (The World Bank, 2013), these conditions make Bangladesh a prime candidate for being the source of newly emerging influenza strains with pandemic causing potential. Therefore, it is vital to enhance our understanding of the factors in Bangladesh that enable currently circulating influenza subtypes (e.g. H5N1) to be both continually transmitted between poultry and occasionally spillover across the human-animal interface. Bangladesh specific risk analyses have determined a number of biosecurity related risk factors associated with H5N1 infection in commercial poultry (Biswas et al., 2009a; Osmani et al., 2014a), while identifying free grazing duck and duck-rice cultivation interacted ecology as not being significant determinants (Gilbert et al., 2010; Ahmed et al., 2012). Risk factors specific to backyard chickens have also been investigated (Biswas et al., 2009b). Osmani et al. (2014b) found the spread of highly pathogenic avian influenza H5N1 in Bangladesh to be characterised by reported long-distance translocation events, with the relative contribution of trade and the market chain versus wild birds in spreading the disease still to be resolved. Loth et al. (2010) investigated temporal and spatial patterns of H5N1 poultry outbreaks in Bangladesh, occurring between March 2007 and July 2009, and their relationship with several spatial risk factors at a sub-district level. Human population density, commercial poultry population density and number of roads per sub-district were found to be significantly associated with H5N1 virus outbreaks. However, they emphasise that research on the roles of wildlife, migratory birds and ducks in the epidemiology of H5N1 in Bangladesh is urgently needed. How the risk of H5N1 infection varies at different spatial resolutions must also be determined, from local administrative units (in Bangladesh referred to as districts), to province level (referred to as divisions), up to the country level. This work focuses on the district level and division level.

To date, very few zoonotic disease dynamic models incorporate zoonotic transmission from the animal reservoir to humans (Lloyd-Smith et al., 2009). In particular, mathematical modelling of H5N1 thus far has generally only quantified poultry transmission parameters (Tiensin et al., 2007; Bouma et al., 2009). Whilst recent seroprevalence and seroconversion studies have been undertaken in poultry workers in Thailand (Dejpichai et al., 2009) and Bangladesh (Nasreen et al., 2015), the work outlined has predominately considered H5N1 infection in livestock only. Devising a new generation of approaches to model cross-species spillover transmission is one of the several challenges related to modelling the emergence of novel pathogens that requires attention (Lloyd-Smith et al., 2015).

The purpose of this study is to outline a modelling framework that incorporates zoonotic transmission at the human–poultry interface, in addition to within-poultry disease dynamics. The model will be utilised to ascertain whether the size and spatial distribution of commercial poultry H5N1 cases in specified regions of Bangladesh can be predicted accurately at different administration levels and, if so, the crucial modelling considerations that are necessary for this to be achieved. Furthermore, we analyse whether the main contributor to the spillover of H5N1 influenza from poultry to humans in Bangladesh, between H5N1 prevalence in the commercial poultry population or other factors (such as interactions at live bird markets (LBMs)), can be distinguished. The findings that arise motivate further studies examining the effectiveness of intervention measures aiming to minimise the risk of zoonotic transmission of H5N1 influenza.

2. Methods

2.1. The data

The data utilised were comprised of four main components: (i) a commercial poultry premises census, (ii) poultry case data, (iii) external risk factors (live bird markets, free-grazing ducks, presence of water, rice cropping), (iv) human case data.

2.1.1. Commercial poultry premises census

In 2010, the Bangladesh office of the Food and Agriculture Organisation of the United Nations (FAO/UN) undertook a census of all commercial poultry premises, listing 65,451 premises in total, of which 2,187 were LBMs. Each premises was visited once, with the premises location recorded along with the number of the following types of avian livestock present during the visit: layer chickens, broiler chickens, ducks, others (e.g. turkeys, quails). Within the census data there were instances of multiple premises having the same location (i.e. identical latitude and longitude coordinates). For these occurrences the avian livestock populations were amalgamated, giving a single population for each category at each location.

Of the non-market locations, 23,412 premises had blank entries for all avian types. It has been confirmed this did correspond to no poultry being present on these premises when the census visit occurred, due to the premises either being between poultry stocks or being temporary closed by the farmer due to an ownership transfer taking place, rather than data entry errors (M.G. Osmani, personal communication). We made a simplifying assumption that at any given time an equivalent proportion of premises would not have any avian livestock at the premises. Therefore, we did not make use of these locations in our analysis. While not discussed here the sensitivity of model outputs to this assumption requires further consideration.

Please cite this article in press as: Hill, E.M., et al., Modelling H5N1 in Bangladesh across spatial scales: Model complexity and zoonotic transmission risk. Epidemics (2017), http://dx.doi.org/10.1016/j.epidem.2017.02.007

Table 1
Breakdown of H5N1 HPAI poultry epidemic waves in Bangladesh.

	Start month	End month	Reported cases
Wave 1	March 2007	July 2007	55
Wave 2	September 2007	May 2008	232
Wave 3	November 2008	June 2009	37
Wave 4	January 2010	June 2010	31
Wave 5	January 2011	May 2011	161
Wave 6	November 2011	April 2012	26

Start month, end month and number of reported infected premises in each of the H5N1 poultry epidemic waves in Bangladesh. In addition to the cases within each wave listed above, the following reported cases occurred between waves: one case in September 2008; two cases in August 2009; one case in June 2001; four cases in August–September 2011; four cases in October 2012–March 2013.

2.1.2. Poultry case data

From 2007 to 2012 inclusive there have been 554 poultry premises with reported H5N1 infection in Bangladesh. These were predominately commercial premises (497 cases), with 57 cases reported from backyard flocks. The Bangladesh office of FAO/UN provided a dataset of confirmed infected premises up to June 2011. Cases occurring after June 2011 were obtained from the OIE World Animal Health Information Database (WAHID) Interface (OIE, 2013). For the case data provided by the latter source we were informed that the Department of Livestock Services reported regularly to WAHID regarding HPAI outbreaks in Bangladesh, with this usually occurring within 24 hours according to the code of the World Organisation for Animal Health (M.G. Osmani, personal communication). We therefore presumed WAHID contained all reported Bangladesh HPAI event information.

For each infected premises the data documented its spatial location, the date that infection was reported, the date of culling, and the total number of poultry infected and culled. We divided the infected premises data into distinct epidemic waves. These were estimated by looking for significant gaps between premises infection dates, with a gap of two months or more used to signify the end of one wave and the start of a new one. The dates and number of cases for each wave are displayed in Table 1.

There were 52 poultry premises recorded as being infected that were not part of the 2010 premises census. When analysing a specific wave all additional entries that occurred during that wave were considered, including the reported backyard farm cases when applicable. In addition, for premises infected during a specific wave we modified the poultry populations to match the flock sizes reported in the poultry case dataset (rather than using the reported values from the 2010 census).

2.1.3. External risk factors

In addition to LBMs (Nasreen et al., 2015), presence of free grazing ducks, water and rice paddy fields have been determined as H5N1 avian influenza risk factors for poultry in other areas of southeast Asia (Gilbert et al., 2007; Van Boeckel et al., 2012). Thus, to investigate the importance of these ecological covariates our most complex models included information on these factors. Duck density at a 1km resolution was obtained from the Gridded Livestock of the World (GLW 2.0) dataset (Robinson et al., 2014). Presence of water bodies was determined from global land cover maps produced by GlobCover at a 300m spatial resolution (Arino et al., 2012). Rice paddy agriculture and cropping intensity in Asia can be routinely mapped and monitored using images from the moderate resolution imaging spectroradiometer (MODIS) sensor onboard the NASA Terra satellite (Xiao et al., 2005, 2006; Zhang et al., 2015). The satellite-based algorithms permit the production of maps and monitoring of cropping intensity and the crop calendar (planting and harvesting dates). This source provided rice paddy coverage in Bangladesh at a 500m spatial resolution for the years 2008 and 2011.

2.1.4. Human case data

There have been eight reported human cases of H5N1 infection, causing one death (World Health Organisation, 2016). Latitude and longitude co-ordinates for these cases were obtained using the FAOs Global Animal Disease Information System (EMPRES-i) database (FAO, n.d.). Seven of the eight human cases occurred within the poultry epidemic waves outlined above. Of these, six were located in the Dhaka division and five within the Dhaka district, with the following distribution of cases across the poultry epidemic waves: one in wave 2, two in wave 5, three in wave 6.

2.2. Poultry model

2.2.1. Selection of spatial scales and epidemic waves

With the majority of human cases being located within the Dhaka district (area: 1,464 km^2) and Dhaka division (in 2010, total area 41,761.8 km^2), our model was focused on these two differing administration (spatial) levels. Further, Dhaka district was of notable interest due to being only one of two districts (out of 18 districts in the Dhaka division) that reported presence of H5N1 infection in all six epidemic waves. For applying our poultry model framework (performing parameter inference) we focused on the epidemic waves containing both human cases and over 100 premises reporting H5N1 infection in poultry. These were wave 2 (September 2007–May 2008) and wave 5 (January 2011–May 2011).

Specifically for the Dhaka district our analysis of waves 2 and 5 considered 1,271 and 1,270 premises, with H5N1 infection in poultry confirmed at 22 and 25 premises respectively. In particular, four out of the six sub-districts comprising the Dhaka district had presence of infection in both waves (Fig. 1).

For the Dhaka division, our wave 2 dataset contained 13,369 premises while the wave 5 dataset contained 13,359 premises. There were 109 and 75 reported cases in waves 2 and 5 respectively, with specific sub-districts having a notably higher proportion of total infection (see Fig. 2). Overall, 18 sub-districts (out of 113 contained within the Dhaka division) had confirmed cases during both waves of interest, with 41 and 25 individual sub-districts having infection present during waves 2 and 5 respectively. Note that owing to the small number of premises recorded as having ducks or other poultry types present, with only two such premises in the Dhaka district and roughly 20 premises in the Dhaka division, we focused on layer and broiler chickens in our poultry models.

The candidate models described below were fitted at the district and division administration levels. However, it is possible that a poultry epidemic had begun in Bangladesh outside the specified region, and/or continued in another region of Bangladesh after the final case was culled in the specified region. To address this, for each spatial level and wave of interest we considered two different sets of dates. The first was a region-specific epidemic time period. This began on the day poultry cases initially occurred in the region of interest, ending on the day the final infected premises was culled. If required, a second epidemic wave time period took the country-wide dates for that epidemic wave. Initial notification and final culling dates for each combination of administration level and wave are provided in Table S1. Finally, for each reported premises the time delay between notification and culling was recorded in the data.

2.2.2. Model structure

We formulated our candidate models as discrete-time compartmental models. At any given point in time a premises *i* could

Please cite this article in press as: Hill, E.M., et al., Modelling H5N1 in Bangladesh across spatial scales: Model complexity and zoonotic transmission risk. Epidemics (2017), http://dx.doi.org/10.1016/j.epidem.2017.02.007

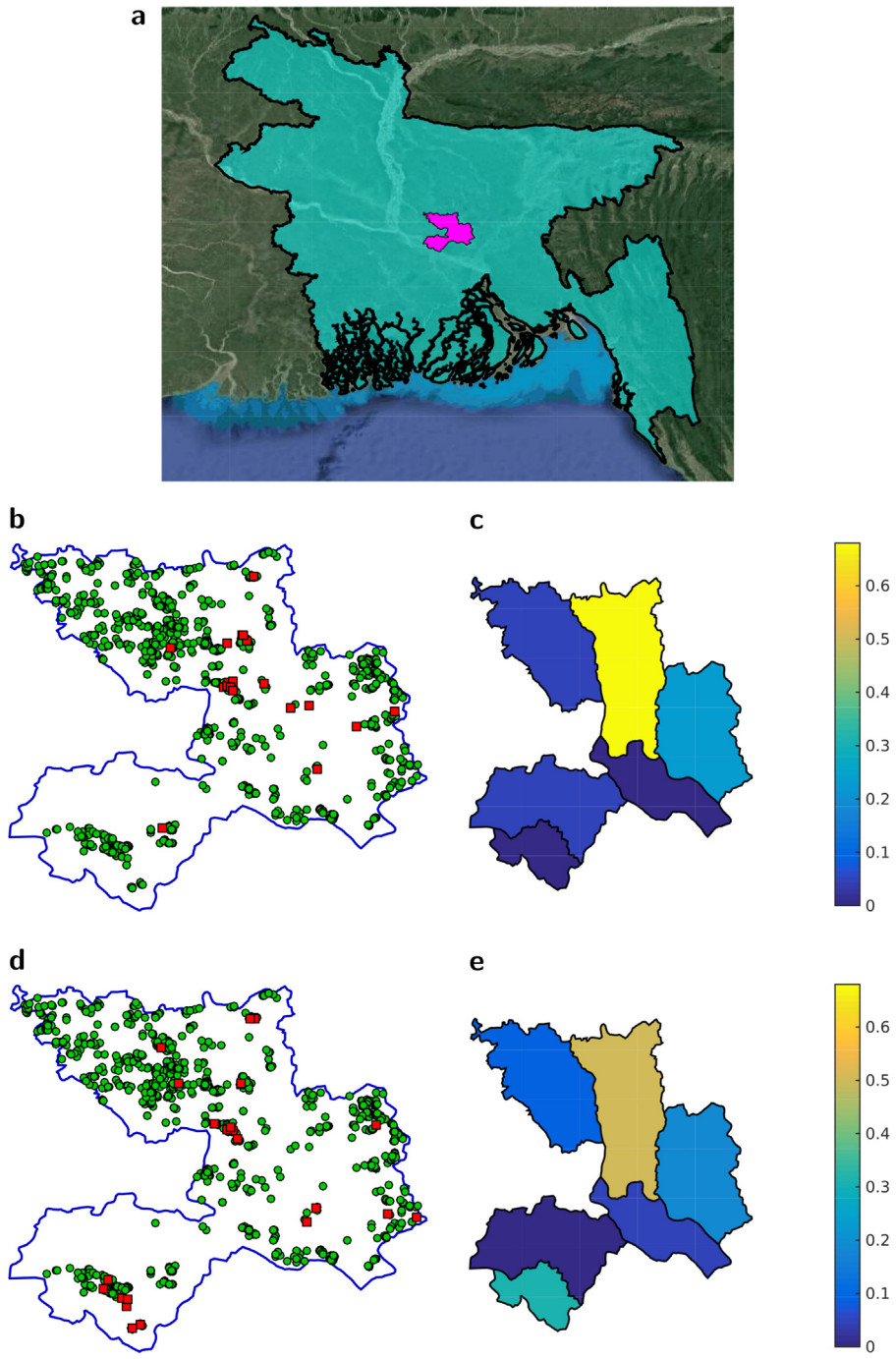

Fig. 1. Spatial locations of premises infected during the wave 2 and wave 5 poultry epidemic waves, located within the Dhaka district. (a) Locator map depicting the location of Dhaka district, shaded in magenta, within Bangladesh, shaded in cyan. (b–e) The left column shows infection status of each premises, with red squares depicting premises that were infected and green circles those that remained susceptible. The right column shows the proportion of infection aggregated at a sub-district level. (b, c) Wave 2 district; (d, e) wave 5 district. (For interpretation of the references to colour in this figure legend, the reader is referred to the web version of the article.)

be in one of four states, S, I, Rep or C: $i \in S$ implies premises i was susceptible to the disease; $i \in I$ implies premises i was infectious and not yet reported; $i \in Rep$ implies premises i was still infectious, but had been reported; $i \in C$ implies that premises i had been culled.

We considered an overall poultry population at each premises (i.e. layer and broiler chickens were not treated as distinct poultry types). This is based on a conceptualisation where the individual poultry enterprise (premises) is the epidemiological unit of interest. In other words, all poultry types within a premises become rapidly infected such that the entire premises can be classified as Susceptible (S), Infected (I), Reported (Rep) or Culled (C). We define a premises i in one of these four states at time t as being in the sets $S(t)$, $I(t)$, $Rep(t)$ or $C(t)$ respectively. While the poultry epidemic was ongoing we assumed a premises was not repopulated once culled.

2.2.3. Notification delays

Our modelling framework incorporated a reporting delay to take into account a premises being infectious before clinical signs of H5N1 infection are observed, which may not be immediate (Biswas et al., 2011), followed by the time taken for premises owners to notify the relevant authorities (FAO, 2011). We treated the delay time as an integer and found that the distributions of other model

Please cite this article in press as: Hill, E.M., et al., Modelling H5N1 in Bangladesh across spatial scales: Model complexity and zoonotic transmission risk. Epidemics (2017), http://dx.doi.org/10.1016/j.epidem.2017.02.007

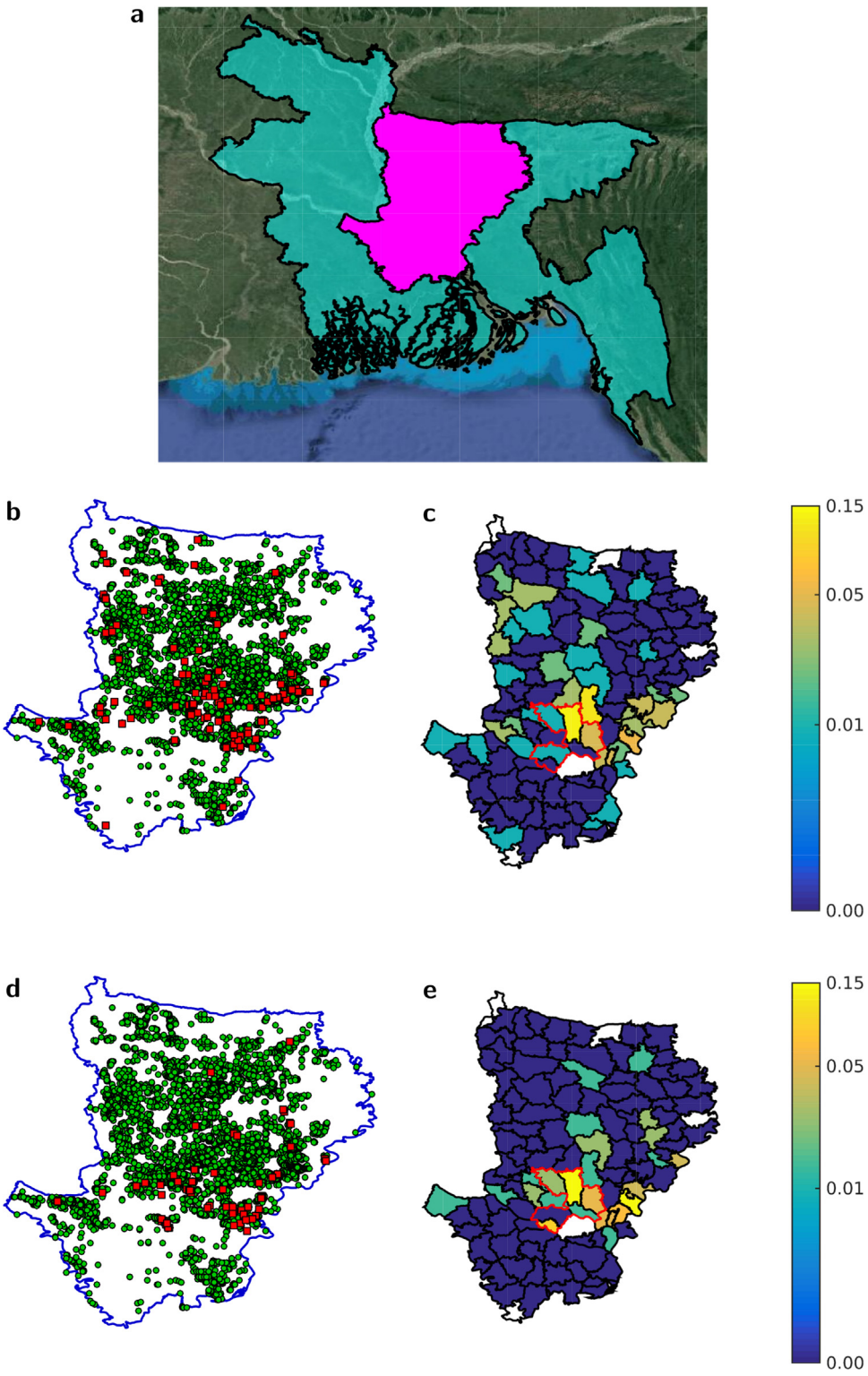

Fig. 2. Spatial locations of premises infected during the wave 2 and wave 5 poultry epidemic waves, located within the Dhaka division. (a) Locator map depicting the location of Dhaka division, shaded in magenta, within Bangladesh, shaded in cyan. (b–e) The left column shows infection status of each premises, with red squares depicting premises that were infected and green circles those that remained susceptible. The right column shows the proportion of infection aggregated at a sub-district level. In (c, e) Dhaka district is outlined in red to highlight its location within the Dhaka division. (b, c) Wave 2 division. (d, e) Wave 5 division. (For interpretation of the references to colour in this figure legend, the reader is referred to the web version of the article.)

parameters were quite sensitive to it. This made it natural to treat different plausible values for the delay as different models, and to select between them (as was done, for example, in the context of selection from discrete outbreak source locations by Hancock et al. (2014)). We chose three fixed infection notification times of two, four and seven days, corresponding to the 50%, 75% and 90% percentiles of the reporting delay distribution for 2009 H5N1 HPAI reports of domestic poultry infection (Farnsworth et al., 2010). We systematically compared model fit and predictions under these different values.

Please cite this article in press as: Hill, E.M., et al., Modelling H5N1 in Bangladesh across spatial scales: Model complexity and zoonotic transmission risk. Epidemics (2017), http://dx.doi.org/10.1016/j.epidem.2017.02.007

2.2.4. Force of infection

The force of infection towards a susceptible premises could be dependent on a variety of factors. Therefore, we proposed a series of nested models of increasing complexity. The base model used is an adaptation of a foot-and-mouth disease model developed by Keeling et al. (2001). The rate at which an infectious premises j infects a susceptible premises i is given by

$$\eta_{ij} = s_c N_{c,i} \times t_c N_{c,j} \times K(d_{ij}), \quad (1)$$

where $N_{c,i}$ is the total number of chickens recorded as being on premises i; s_c and t_c measure the individual chicken susceptibility and transmissibility; d_{ij} is the distance between premises i and j in kilometres; and K is the transmission kernel to capture how the relative likelihood of infection varies with distance.

We extended the model by including a "spark" term parameter ϵ_i to allow for spontaneous, non-distance dependent infections that were unexplained by the susceptibility, transmissibility and kernel components of the model (Deardon et al., 2010). In combination with the distance-dependent transmission kernel, K, this allows our model framework to capture premises contacts that are both dependent on, and independent of, distance. In the absence of empirical poultry movement data, such an approach (including separate distance-dependent and distance-independent terms) has been found to be preferred for modelling animal movement contact data compared to a solely distance dependent process (Lindström et al., 2009). Further, despite the absence of explicit data on backyard poultry its contribution to the force of infection could be incorporated into ϵ_i.

Overall, the force of infection against a susceptible premises i on day t ($\text{Rate}_M(i,t)$ for model label M) was comprised of two terms: (i) the force of infection generated by an infectious premises j ($\eta_{ij,M}$), (ii) the spark term ($\epsilon_{i,M}$). As a result, the total force of infection has the following general form for model M:

$$\text{Rate}_M(i,t) = \left(\sum_{j \in I(t) \cup Rep(t)} \eta_{ij,M} \right) + \epsilon_{i,M}.$$

We now outline the key constituents of our proposed nested models for the force of infection, labelled A to E. We give a full mathematical description of the baseline model (model A) below. Subsequent models build upon one another through the inclusion of additional parameters, with mathematical descriptions of the remaining models provided in the Supplementary Material.

Baseline model (A)

For the baseline model (model A) the infected premises contribution to the force of infection matched the Keeling et al. (2001) model (Eq. (1)),

$$\eta_{ij,A} = s_c N_{c,i} \times t_c N_{c,j} \times K(d_{ij}).$$

In this case K was derived from the Dhaka division poultry case data. For each infected premises we found the nearest premises that was infected within the previous two days before that farm was reported. The distance between the infecting premises and the newly infected premises was calculated, with the process repeated for each infected premises. Kernel density estimation (KDE) was applied, via the Matlab function `kde()`, to the distances obtained from this process. This approximated a smooth functional form for K.

The spark term was the same fixed value for every premises, $\epsilon_{i,A} = \epsilon$. Subsequently, the total rate of infection against a susceptible premises i on day t satisfied

$$\text{Rate}_A(i,t) = \left(\sum_{j \in I(t) \cup Rep(t)} \eta_{ij,A} \right) + \epsilon. \quad (2)$$

To make the model identifiable we set $s_c = 1$. This is carried forward in all subsequent models. Note that although this changes the interpretation of the parameters, it does not have any epidemiological implications.

This left two parameters in (2) requiring estimation, t_c and ϵ.

Parametric kernel model (B)

For the parametric kernel model (model B) we fit a parametric transmission kernel K in place of the kernel derived from the poultry case data. Our chosen transmission kernel was pareto distributed, with a single parameter $\alpha \geq -1$. This kernel form could provide insights into how transmission risk varied with respect to the distance between the infected premises and target susceptible location. Values of α close to -1 would give a relatively constant kernel over all distances, with $\alpha = -1$ corresponding to transmission risk being independent of distance. As α increases away from -1 localised transmission is favoured, with long-range transmission diminished.

With this set up the following three parameters were fitted: t_c, α, ϵ.

Nonlinear farm size model (C)

Previous modelling work on foot-and-mouth disease in the UK suggests including parameters that account for a non-linear increase in susceptibility and transmissibility as animal numbers on a premises increase provide a closer fit to historical epidemic data than when these powers are set to unity (Deardon et al., 2010; Tildesley et al., 2008). We explored whether this behaviour applied to H5N1 avian influenza by adding power law exponents to the susceptible population, p_c, and infected population, q_c. This gave five parameters to be estimated (t_c, α, ϵ, p_c, q_c).

Full ecological model (D)

For each spatial level and epidemic wave, the preferred model out of models A–C was ascertained by comparing deviance information criterion (DIC) values (see model comparison methodology). The preferred model was carried forward with the single premises-independent spark term ϵ replaced by four ecologically motivated spark term covariates to form model D. In detail, these were the presence or absence of the following in the neighbourhood of the given premises, with the resolution used for each covariate stated in brackets: (i) water bodies (300 m grid); (ii) paddy fields (500 m grid); (iii) LBMs (within 5 km); (iv) local ducks (1 km grid). The rice paddy data was taken from the same year the epidemic wave of interest took place (i.e. from 2008 if considering a wave 2 model and from 2011 if considering a wave 5 model).

Simple ecological model (E)

Despite a number of studies identifying domestic waterfowl and rice crop intensity having a strong association with HPAI H5N1 presence (Gilbert et al., 2007; Van Boeckel et al., 2012; Gilbert and Pfeiffer, 2012), previous work has determined these factors as not being significant within Bangladesh (Gilbert et al., 2010; Ahmed et al., 2012). Due to this, we considered a simplified ecological model that contained only the presence or absence of water bodies and LBMs (in the same manner outlined above for the full ecological model) in the neighbourhood of the given premises as ecological spark term covariates.

Once more, for each spatial level and epidemic wave we carried forward the preferred model out of models A–C and added the additional spark term covariates to form model E.

Please cite this article in press as: Hill, E.M., et al., Modelling H5N1 in Bangladesh across spatial scales: Model complexity and zoonotic transmission risk. Epidemics (2017), http://dx.doi.org/10.1016/j.epidem.2017.02.007

2.3. Parameter estimation

Parameter estimation was carried out within a Bayesian framework, with the parameter posterior distribution (given the observed data) explored via Markov chain Monte Carlo (MCMC) using the slice sampling method (Neal, 2003) or adaptive Metropolis parameter updates (Haario et al., 2001). We assumed uniform priors for all our parameters: $t_c \sim \mathcal{U}(0, 0.1)$; $\alpha \sim \mathcal{U}(-1, 10)$; $p_c \sim \mathcal{U}(0, 2)$; $q_c \sim \mathcal{U}(0, 2)$; $\epsilon \sim \mathcal{U}(0, 1)$; $\epsilon_{\text{water}} \sim \mathcal{U}(0, 1)$; $\epsilon_{\text{rice}} \sim \mathcal{U}(0, 1)$; $\epsilon_{\text{LBM}} \sim \mathcal{U}(0, 1)$; $\epsilon_{\text{ducks}} \sim \mathcal{U}(0, 1)$. Full details of the likelihood function used in this analysis are given in the Supplementary Material.

2.4. Model comparison methodology

To compare models of the same type, differing only by the value of the reporting delay, we used deviance information criterion (DIC) (Spiegelhalter et al., 2002; Gelman et al., 2003), calculated using the samples generated from our MCMC simulations. We chose to predict the notification time (reporting delay) based on the DIC in order to account for differences in the effective number of parameters of the fitted models, with the fixed time that gave the lowest DIC being preferred.

Further, after selecting the reporting delay that should be used for each of our models, DIC was used again to compare our set of nested models (at a given spatial level for a specific poultry epidemic wave). This was due to its capability of accounting for additional parameters increasing model complexity. While models with smaller DIC were preferred over models with larger DIC, note that models with a DIC value within two of the model with the lowest DIC value still deserved consideration, while being at least three greater meant there was considerably less support for that model given the data (Spiegelhalter et al., 2002). Further information regarding DIC can be found in the Supplementary Material.

2.5. Zoonotic transmission model

A simple zoonotic transmission model was constructed to fit to the temporal human case data. We focused solely on the within-region epidemic time period. The rate of spillover transmission on a given day t, $\lambda(t)$, was chosen to have the following dependencies,

$$\lambda(t) = \beta I_b(t) + \epsilon_h,$$

where β is the poultry to human transmission rate, $I_b(t)$ is the number of infected poultry within the region of interest and ϵ_h is a constant human spark term.

With previous work finding the Poisson distribution provided an adequate goodness of fit to daily human H5N1 case data in Egypt (Rabinowitz et al., 2012), we assumed the occurrence of human cases followed a Poisson process. As a result, the waiting time until the next human case occurrence followed an exponential distribution. The probability of a human infection event occurring in the next day (i.e. $\delta t = 1$) was given by

$$h_t = 1 - e^{-\lambda(t)}.$$

Over the entire poultry epidemic a likelihood function for human case occurrence, L_h, could be constructed,

$$L_h = \left(\prod_{i \in D_{\text{inf}}} (h_i) \right) \left(\prod_{j \in D_{\text{sus}}} (1 - h_j) \right), \tag{3}$$

with D_{inf} the set of days a human case occurred and D_{sus} the set of days there were no human cases. In detail, the first term corresponds to the probability of a human case occurring on days where the human case data reported at least one person becoming infected, with the second term giving the probability that no human cases occurred on all other days. Subsequently, the log-likelihood $\log(L_h)$ could be derived:

$$\log(L_h) = \left(\sum_{i \in D_{\text{inf}}} \log(h_i) \right) + \left(\sum_{j \in D_{\text{sus}}} \log(1 - h_j) \right), \tag{4}$$

With human cases only occurring in epidemic waves 2, 5 and 6, we applied our model to these waves only. Relationships between β and ϵ_h were analysed by producing log-likelihood surfaces using (4), with parameter summary statistics inferred using MCMC with adaptive Metropolis updates (Haario et al., 2001). The following uniform prior distributions were used for each parameter: $\beta \sim \mathcal{U}(0, 1)$, $\epsilon_h \sim \mathcal{U}(0, 1)$.

2.6. Model verification

To verify the validity of our model fitting we performed stochastic simulations, checking the correspondence of temporal and spatial summary statistics with the observed data. Our simulated poultry model was a spatial individual-based model at the premises level. It incorporated both the Tau-leap algorithm (Gillespie, 2001), allowing multiple events to occur each time step, and a grid-based approach outlined by Keeling and Rohani (2008). In addition, we accounted for zoonotic transmission over the entire poultry epidemic in each simulation.

We carried out 1000 simulation runs for each model. Both model components used distinct sampled parameter values, obtained previously via MCMC, in each run. The number of time steps matched the length of the epidemic wave the particular model had been fitted to. For the models fitted using region-specific epidemic dates we initialised the simulation with a single infected premises, corresponding to the location first reporting infection for that respective epidemic wave and spatial level. For the models fitted using country-wide epidemic dates all premises were initialised as susceptible. For infected premises the time between reporting and culling was randomly sampled from the observed reporting to culling time empirical probability mass function.

For both premises and human cases our first goodness-of-fit check was to compare the distribution of simulated final epidemic sizes to the observed data. For the poultry model we also inspected reported case temporal profiles to ensure our simulations produced similar behaviour.

A separate class of goodness-of-fit tests focused on spatial aspects. First order spatial patterns were compared by computing the difference between a density surface of the observed case locations and a density surface of the predicted case locations averaged over 1% of simulations with the largest aggregate two-dimensional correlation with the data (when aggregated by sub-district). Further, we used Ripley's K function (Ripley, 1976, 1977) to ascertain whether the measure of clustering in the spatial pattern of observed infected premises could be plausibly generated by our fitted models. To assess whether premises-to-premises transmission could be sustained without the need for importations, or infections derived from external sources, we computed premises-level basic reproductive ratios (Tildesley and Keeling, 2009). This determined the expected number of other premises the given premises would infect if infected itself. Those premises with the greatest transmission potential would therefore be highlighted. Further details of the Ripley's K function and premises-level reproductive ratio are described in Supplementary material.

We also assessed how accurately model parameters could be inferred from the data. To do this we performed simulations using sample outputs from the MCMC model fitting procedure, with each set of simulated data fitted to the same model it had been generated

Please cite this article in press as: Hill, E.M., et al., Modelling H5N1 in Bangladesh across spatial scales: Model complexity and zoonotic transmission risk. Epidemics (2017), http://dx.doi.org/10.1016/j.epidem.2017.02.007

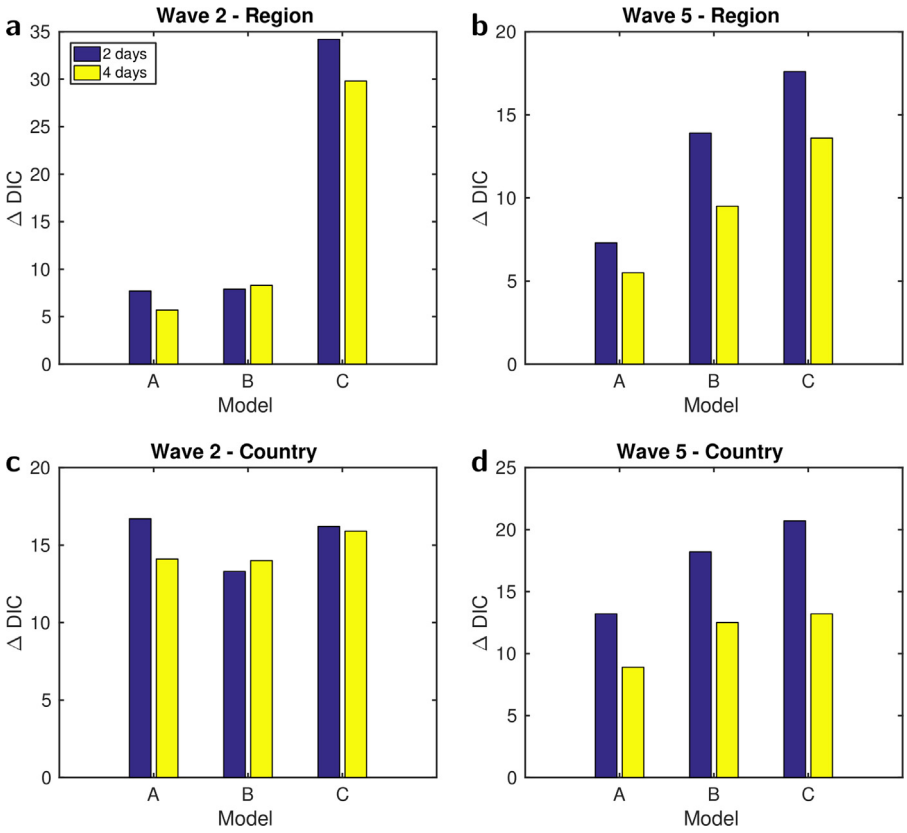

Fig. 3. Bar plots comparing ΔDIC values for the district datasets fitted to our models with various fixed infected to reporting times. For each model a reporting delay of seven days gave the minimum DIC value. The depicted ΔDIC is with respect to the version of the model using a seven day infected to reporting time. (a) Wave 2, region-specific epidemic dates; (b) wave 5, region-specific epidemic dates; (c) wave 2, country-wide epidemic dates; (d) wave 5, country-wide epidemic dates.

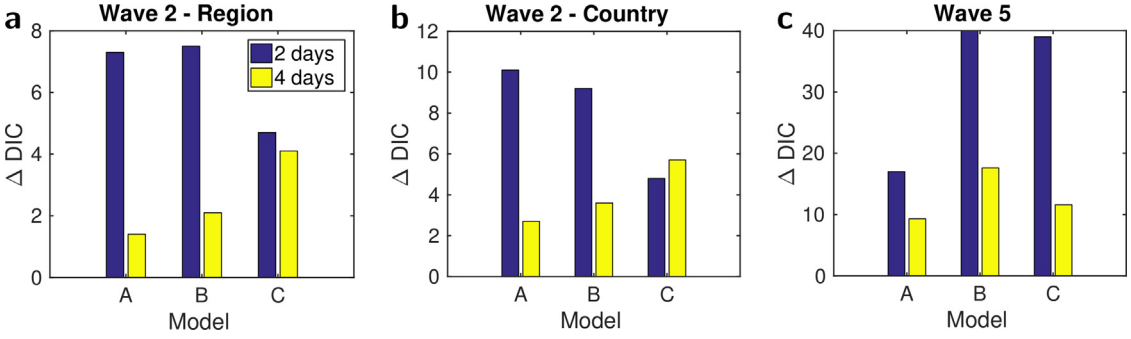

Fig. 4. Bar plots comparing ΔDIC values for the division datasets fitted to our models with various fixed infected to reporting times. For each model a reporting delay of seven days gave the minimum DIC value. The depicted ΔDIC is with respect to the version of the model using a seven day infected to reporting time. (a) Wave 2, region-specific epidemic dates; (b) wave 2, country-wide epidemic dates; (c) wave 5.

from using MCMC methods. The estimated posterior parameter densities were then compared to the "true" value.

All calculations and simulations were performed with MATLAB®.

3. Results

3.1. Poultry model

In our comparison of DIC values for models of the same type, differing only by the value of the reporting delay, a fixed reporting delay of seven days was common across both waves and spatial levels (Figs. 3 and 4, see Tables S2 and S3 for a complete listing of model DIC values). This indicates the reporting of cases during these poultry epidemics was non-optimal.

Consistency in the complexity of the best fit models varied for the two different administration levels of interest (see Table 2 for a listing of preferred models). At the division level the added complexity in the nonlinear farm size model (model C) was preferred, though adding in additional spark terms that were risk factor specific seemingly brought no additional benefits. On the other hand,

Table 2
Preferred models and fixed reporting delay time for each wave and spatial level.

	Epidemic dates	District	Division
Wave 2	Region	Model E/7 days	Model C/7 days
	Country	Model E/7 days	Model C/7 days
Wave 5	Region	Model B/7 days	Model C/7 days
	Country	Model B/7 days	–

Please cite this article in press as: Hill, E.M., et al., Modelling H5N1 in Bangladesh across spatial scales: Model complexity and zoonotic transmission risk. Epidemics (2017), http://dx.doi.org/10.1016/j.epidem.2017.02.007

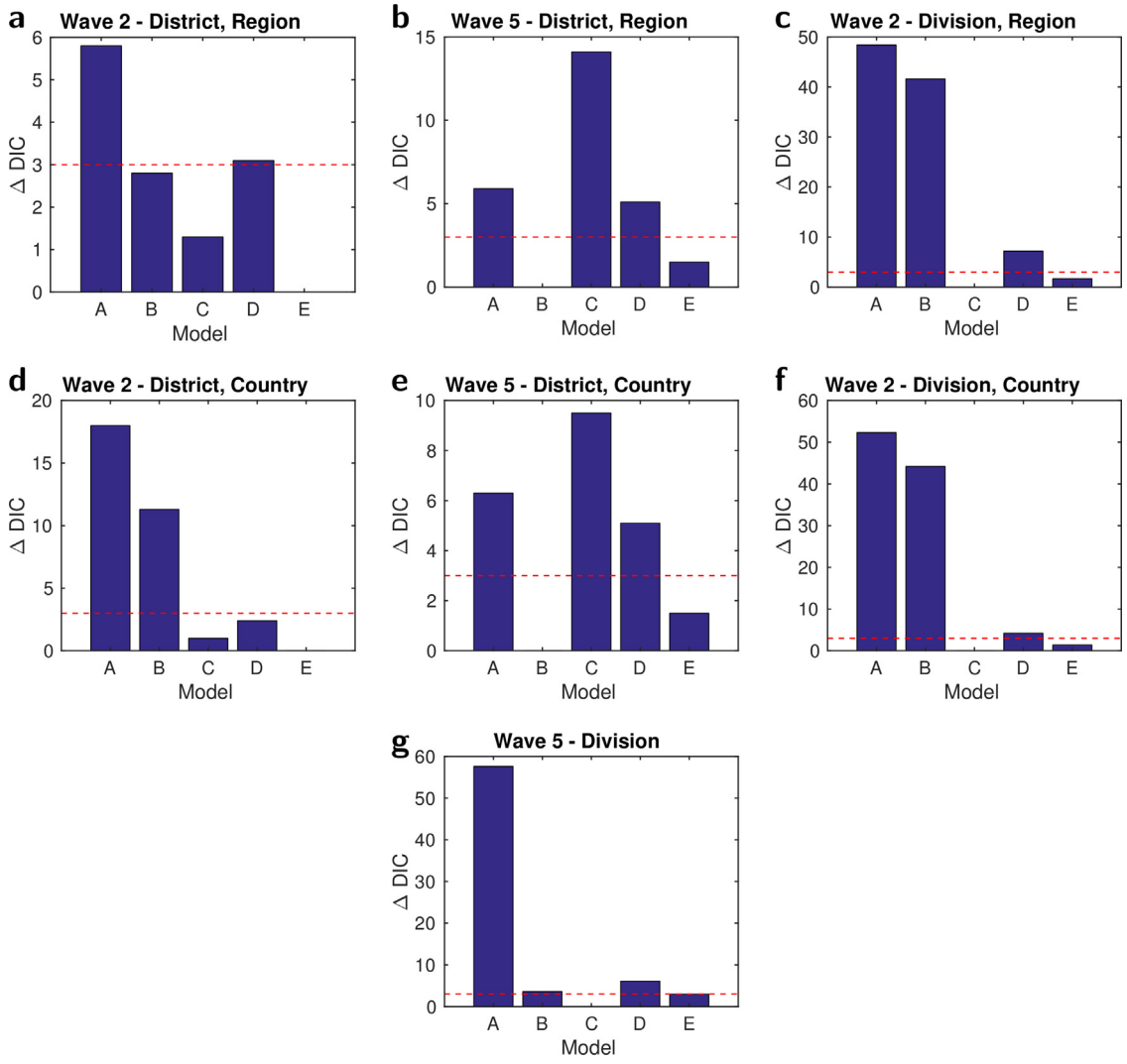

Fig. 5. Bar plots comparing ΔDIC values for the different datasets fitted to our nested models. For each model the fixed reporting delay time that minimised the DIC was used (see Tables S2 and S3). The preferred model had a ΔDIC = 0. Models with $\Delta\text{DIC} \geq 3$ have considerably less support and lie above the red, dashed line. Full DIC values are given in Table S4. (a) Wave 2 district, region-specific epidemic dates; (b) wave 5 district, region-specific epidemic dates; (c) wave 2 division, region-specific epidemic dates; (d) wave 2 district, country-wide epidemic dates; (e) wave 5 district, country-wide epidemic dates; (f) wave 2 division, country-wide epidemic dates; (g) wave 5 division. (For interpretation of the references to colour in this figure legend, the reader is referred to the web version of the article.)

across both waves and sets of epidemic dates the chosen models for our district datasets covered a wider array of the possible model options (Table 2). This implied that differing modelling characteristics were required based on the spatial scale of interest. Fitting to the wave 5 district datasets the parametric kernel model (model B) was preferred. For the wave 2 data, considering only models A–C, the nonlinear farm size model (model C) was chosen. Whilst carrying forward the nonlinear farm size model framework we determined the simple ecological model (model E) as being preferred relative to all candidate models (Fig. 5, see Table S4 for a complete listing of model DIC values).

Though the simple ecological model (model E) was only found to be preferred for the wave 2 district datasets, the majority of the remaining datasets found that this model had a DIC value within two of the DIC value for the best-fit model, meaning such a model was still plausible given the data. In addition, for the majority of our datasets the full ecological model (model D) was found to have considerably less support relative to the simple ecological model (see Table S4).

When comparing parameter summary statistics for our best fit models at the division level (Table 3) and district level (see Tables S5 and S6), a spatial level specific feature was the apparent greater contribution of importations and transmission from other sources (characterised by the ϵ parameters) to the force of infection at the district level versus the division level. On the other hand, the relationship between increasing flock size and premises-level susceptibility was approximately linear (i.e. $p \approx 1$) in both model types (Tables 3, S5 and S6). A reasonable level of identifiability was observed for model parameters, giving extra confidence to our results (see Supplementary Figs. S1 and S2).

Comparing the estimated parameter distributions for our wave 2 and wave 5 division-level models highlights noticeable differences in the factors driving disease spread across the two waves. Of particular interest were discrepancies in α, the transmission kernel parameter, and q, the infected premises population exponent (see Table 3). While for wave 2 α was typically below 0, for wave 5 α was approximately zero, giving a stronger preference towards short-range transmission. For q, fitting to the wave 2 epidemic found approximately equal contributions to the force of infection from each infected premises against a susceptible premises, irrespective of the infected premises population size. In stark contrast, fitting to the wave 5 epidemic we inferred the median value of q to

Table 3
Parameter summary statistics for preferred division models.

		Wave 2		Wave 5
		Region specific	Country-wide	Region specific
	Model	C	C	C
	Inf. to Rep. time (days)	7	7	7
t_c	Mean	1.06×10^{-7}	9.63×10^{-8}	1.71×10^{-10}
	Median	7.70×10^{-8}	7.03×10^{-8}	1.56×10^{-10}
	(95% CI)	$(7.29 \times 10^{-9}, 3.78 \times 10^{-7})$	$(3.71 \times 10^{-9}, 3.42 \times 10^{-7})$	$(5.86 \times 10^{-11}, 3.63 \times 10^{-10})$
ϵ	Mean	4.11×10^{-6}	2.49×10^{-6}	1.04×10^{-5}
	Median	3.98×10^{-6}	2.35×10^{-6}	1.02×10^{-5}
	(95% CI)	$(1.42 \times 10^{-6}, 7.91 \times 10^{-6})$	$(8.80 \times 10^{-7}, 4.80 \times 10^{-6})$	$(5.02 \times 10^{-6}, 1.72 \times 10^{-5})$
α	Mean	−0.358	−0.394	0.0136
	Median	−0.345	−0.377	0.0136
	(95% CI)	(−0.666, −0.159)	(−0.713, −0.172)	(−0.122, 0.143)
p	Mean	1.06	1.05	1.05
	Median	1.06	1.06	1.05
	(95% CI)	(0.923, 1.19)	(0.916, 1.18)	(0.826, 1.26)
q	Mean	0.0574	0.0732	1.06
	Median	0.0427	0.0458	1.06
	(95% CI)	(0.00175, 0.189)	(0.00243, 0.300)	(0.844, 1.28)

Parameter mean, median and 95% credible intervals (CI) from 1,000 samples obtained from MCMC.

be greater than one, implying poultry premises with the largest populations had a significant role in H5N1 transmission.

3.2. Zoonotic transmission model

Log-likelihood surfaces were produced for waves 2, 5, and 6 using (4). Two preferred regions of parameter space were found in general, though there is evidence of parameter dependent threshold values (Fig. 6a and b). Below these threshold values the other parameter dominates the dynamics of the system. When fitting to the wave 5 data there was little dependence upon the spark term ϵ_h, with β playing a much more significant role. In other words, the number of infected birds has some significance in the likelihood of zoonotic transmission occurring. The opposite was found to be true for wave 2, with more importance placed on the human case spark term.

Within wave 6 there were three human H5N1 case occurrences. All three were situated inside the Dhaka division, while two of the three were contained within the Dhaka district. At both spatial levels there was very little dependence on the number of infected poultry, with the spark term ϵ_h being dominant (Fig. 6c and d).

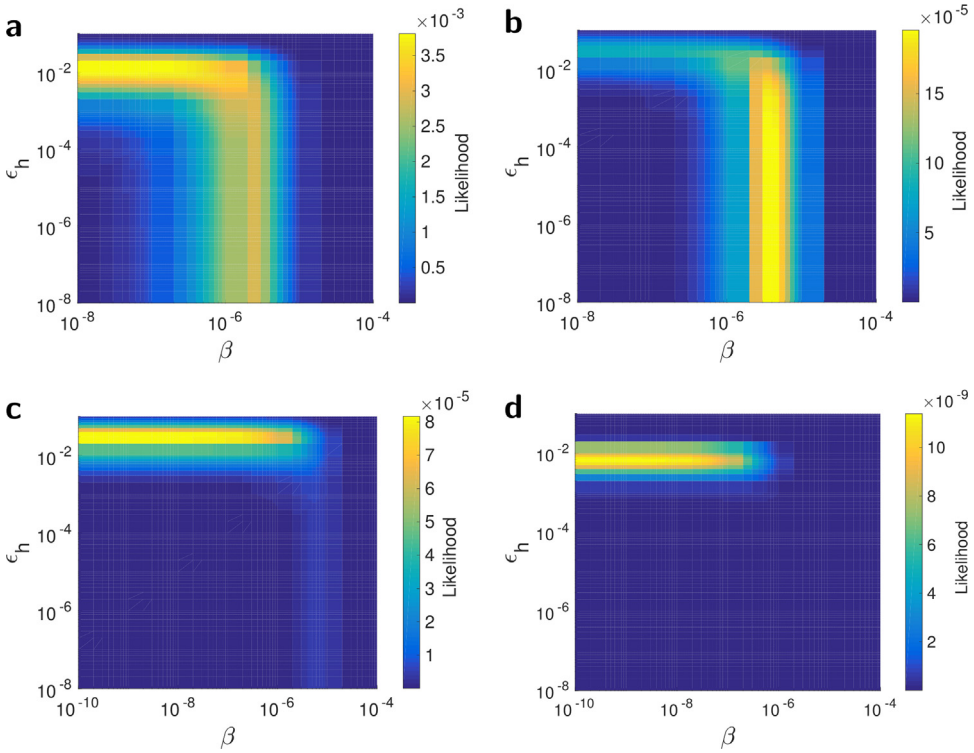

Fig. 6. 2D likelihood surface of temporal zoonotic transmission model parameters. Lighter colours signify a higher likelihood. The preferred regions of parameter space when fitting to the following datasets were: (a) Wave 2 district – the dynamics were dominated by ϵ_h; (b) wave 5 district – little dependence upon the spark term ϵ_h, with β playing a much more significant role; (c, d) wave 6 district and division – the spark term ϵ_h was dominant at both spatial levels. (For interpretation of the references to colour in this figure legend, the reader is referred to the web version of the article.)

Please cite this article in press as: Hill, E.M., et al., Modelling H5N1 in Bangladesh across spatial scales: Model complexity and zoonotic transmission risk. Epidemics (2017), http://dx.doi.org/10.1016/j.epidem.2017.02.007

Parameter summary statistics inferred from approximately 40,000 samples generated via MCMC are stated in Table S7. Premises infection dates were computed from the observed reporting dates using the fixed reporting delay time in the preferred model for the respective wave and spatial level. Acceptance rates were between 20 and 25%. As for the poultry transmission component, we were able to recover unbiased estimates of the zoonotic transmission model parameters from simulated data (Supplementary Figs. S3 and S4).

3.3. Model verification

Simulation output from our district-level models were found to agree favourably with the observed data. Using region-specific epidemic dates the simulated final premises and human epidemic sizes captured the observed data for both waves. This was maintained when considering country-wide epidemic dates, though the distributions for both waves became heavy-tailed (Fig. 7). Further, the observed spatial distribution of infected premises could be plausibly generated by our fitted models (Fig. 8). The simulated models did exhibit a much broader range of possibilities for spatial structure, but the observed data was predominately within the 95% prediction interval (Supplementary Fig. S5). Lastly, the fitted district-level models were capable of generating plausible reported case temporal profiles, which were dominated by single daily cases (Supplementary Fig. S6).

Across the majority of the district models the number of premises with premises-level reproductive ratios estimated to be greater than one was limited. Therefore, infections seeded in a random premises by importations or other ecological factors would more than likely fail to spread (Fig. 9). On the other hand, for both waves small clusters of premises, all with $R_i > 1$, were present in the centre third of the district (and in the south-west and north-west for wave 5). Our results indicate that localised outbreaks would be possible here, corresponding well with the true locations of the wave 5 observed cases in particular (see Fig. 1).

For our division-level models the amount of agreement between the simulated output and the observed data was more variable. Although predictions from the models fitted to the wave 2 data generally underestimated the observed premises epidemic size (Fig. 10), they did generate infection spatial distributions with comparable measures of spatial homogeneity (Fig. 11). In contrast, for wave 5 we obtained a bimodal distribution, with the observed premises epidemic size lying just above the lower valued peak (Fig. 10e). The knock-on effect of this is a widely spanning human case distribution (Fig. 10f). Measures of spatial homogeneity in the spatial pattern of the observed infected premises data could be plausibly generated (Fig. 11c). Although first order spatial correspondence with the case data was not as strong for our fitted division-level models (compared to the district models), a subset of simulation runs could capture the prominent outbreak regions located centrally and on the eastern edge of the division (Supplementary Fig. S7). Temporally, both waves exhibited two typical behaviours. These were either a single large outbreak, or a small outbreak with intermittent spikes in cases that mirrored the true temporal profiles (Supplementary Fig. S6).

Spatially, of particular interest was the wave 5 division model. The observed cases mainly lie in the centre third of the division, spanning the entire width of the region. However, model simulations found the regions infected most often lay further north of this band (Supplementary Fig. S8). Analysis of premises-level reproductive ratios revealed the extent to which a number of premises are theoretically able to transmit infection. Both wave 2 division-level models gave the highest R_i values in a similar area, though these were only just above one and smaller in scale when compared to the wave 5 division-level model (Fig. 12). Furthermore, the wave 2 division-level models predict that the areas capable of continuing a transmission chain are concentrated in a single central region. In contrast, the wave 5 division-level model gave a smaller central region with $R_i > 1$, but indicated extra sporadic areas in the north and south-west with the capability of continuing the chain of transmission if infection arose in those localities (Supplementary Fig. S9).

4. Discussion

This analysis illustrates how altering the spatial scale of interest can revise the factors meriting inclusion in mathematical models of H5N1 HPAI influenza transmission among poultry. For Bangladesh, a preferred model framework was identifiable at the division level, with the nonlinear farm size model (model C) chosen. This implies that fitting a transmission kernel, rather than using a kernel estimated from case data, and allowing for non-linear dependencies in both infecting and susceptible premises population sizes are important inclusions. In contrast, at the district level a preferred model could not be established, suggesting the data were not sufficient to determine the key aspects of a district-level model for general use.

Finding that the simple ecological model (model E) was strongly preferred to the full ecological model (model D) for the majority of our wave and spatial level combinations corroborates previous studies, which found ducks and rice cropping systems were not strongly associated with H5N1 HPAI infection risk in Bangladesh (Gilbert et al., 2010; Ahmed et al., 2012). However, the inclusion of extra parameters (relative to models A–C) was penalised in the DIC calculation, resulting in the simple ecological model (model E) not being considered as the 'best-fitting' of our candidate models for the majority of our datasets. Nonetheless, other ecological covariate dependencies besides linear could have been chosen. Modified conclusions may be drawn with these alternative choices.

By fitting models at both district and division levels we could uncover model characteristics that were independent of spatial scale. Demonstrated by a reporting delay of seven days being persistently selected across the entire nested model range, this is noteworthy in indicating non-optimal reporting of infected premises during these poultry epidemics. Furthermore, finding an approximately linear relationship between increasing flock size and premises-level susceptibility highlights a potential detection bias (as an alternative to the natural interpretation of larger flock sizes having increased risk of exposure), with outbreaks more likely to be reported by large premises. This is in agreement with Osmani et al. (2014a), who hypothesised poor disease detection and reporting within endemically infected regions of Bangladesh as plausible reasons for genetically identical viruses seemingly causing independent outbreaks over moderate time periods (<14 days). Such behaviour is conceivable due to the mortality rate within a flock in the early course of HPAI H5N1 infection being low, meaning detection of such clinical events may be delayed (Biswas et al., 2011).

Detection delays are further compounded by many producers being wary following past experiences with government veterinary services, especially those that carried out mass culling or offered poor compensation for poultry destroyed, further extending the time from initial premises infection to reporting (FAO, 2011). This hinders intervention efforts, with pre-existing strategies to combat H5N1 infection of poultry having a limited impact. For example, a recent H5N1 surveillance study in Bangladesh poultry found no significant difference in anti-H5 seropositivity between vaccinated and unvaccinated chickens, indicating a failure of the vaccination program and a need for updated poultry vaccines (Ansari et al., 2016). Moreover, a practice of weekly rest days at LBMs that started in April 2012 and the introduction of improved

Please cite this article in press as: Hill, E.M., et al., Modelling H5N1 in Bangladesh across spatial scales: Model complexity and zoonotic transmission risk. Epidemics (2017), http://dx.doi.org/10.1016/j.epidem.2017.02.007

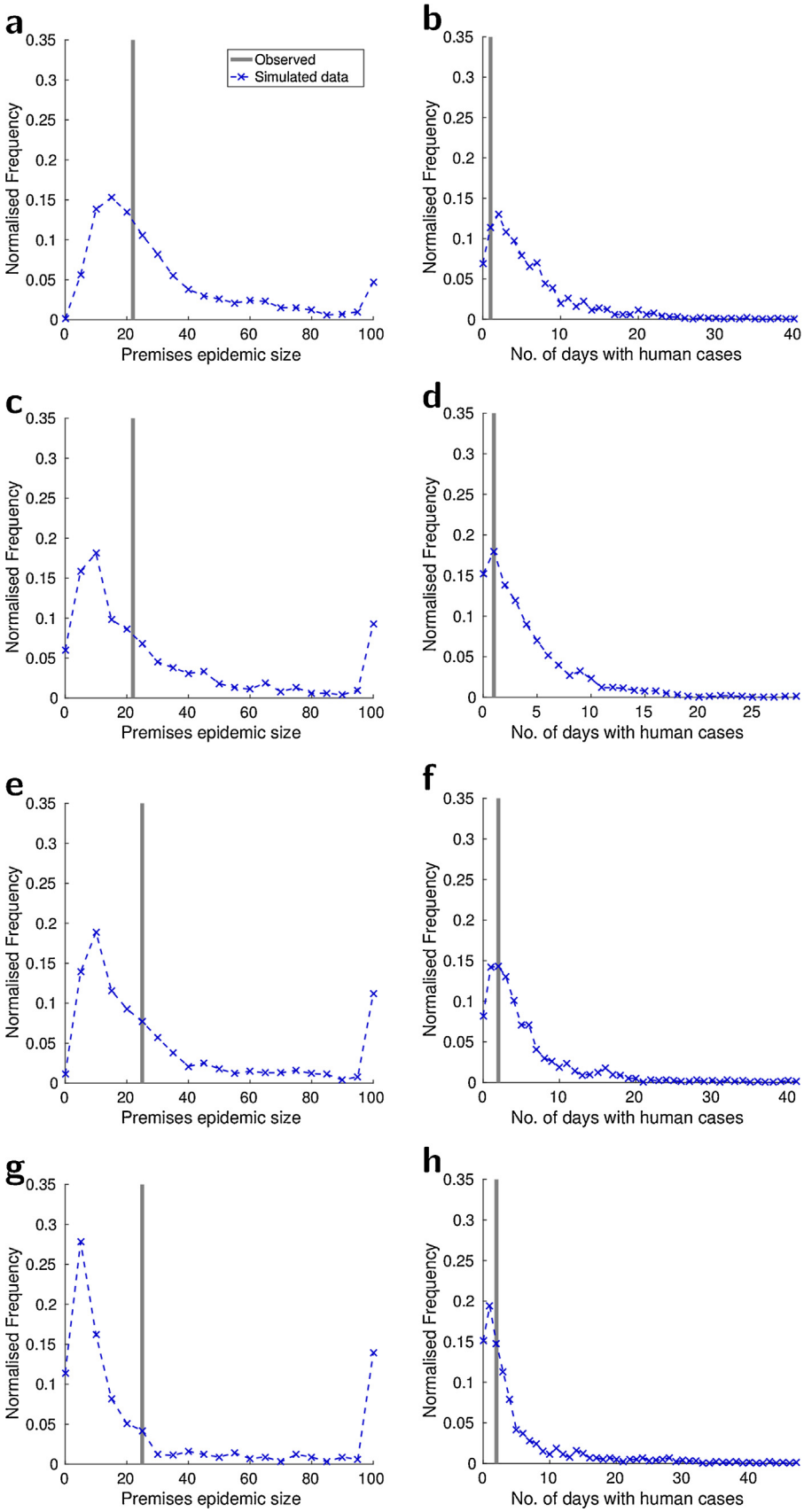

Fig. 7. Simulated premises epidemic size and human case occurrence versus observed data at the district level. Left column shows the premises epidemic size versus the observed data for each of our district datasets. Similarly, the right column shows simulated human case occurrence verses the observed data. (a, b) Wave 2, region-specific epidemic dates; (c, d) wave 2, country-wide epidemic dates; (e, f) wave 5, region-specific epidemic dates; (g, h) wave 5, country-wide epidemic dates. The normalised frequency at 100 also includes all epidemic sizes 100 or greater.

Please cite this article in press as: Hill, E.M., et al., Modelling H5N1 in Bangladesh across spatial scales: Model complexity and zoonotic transmission risk. Epidemics (2017), http://dx.doi.org/10.1016/j.epidem.2017.02.007

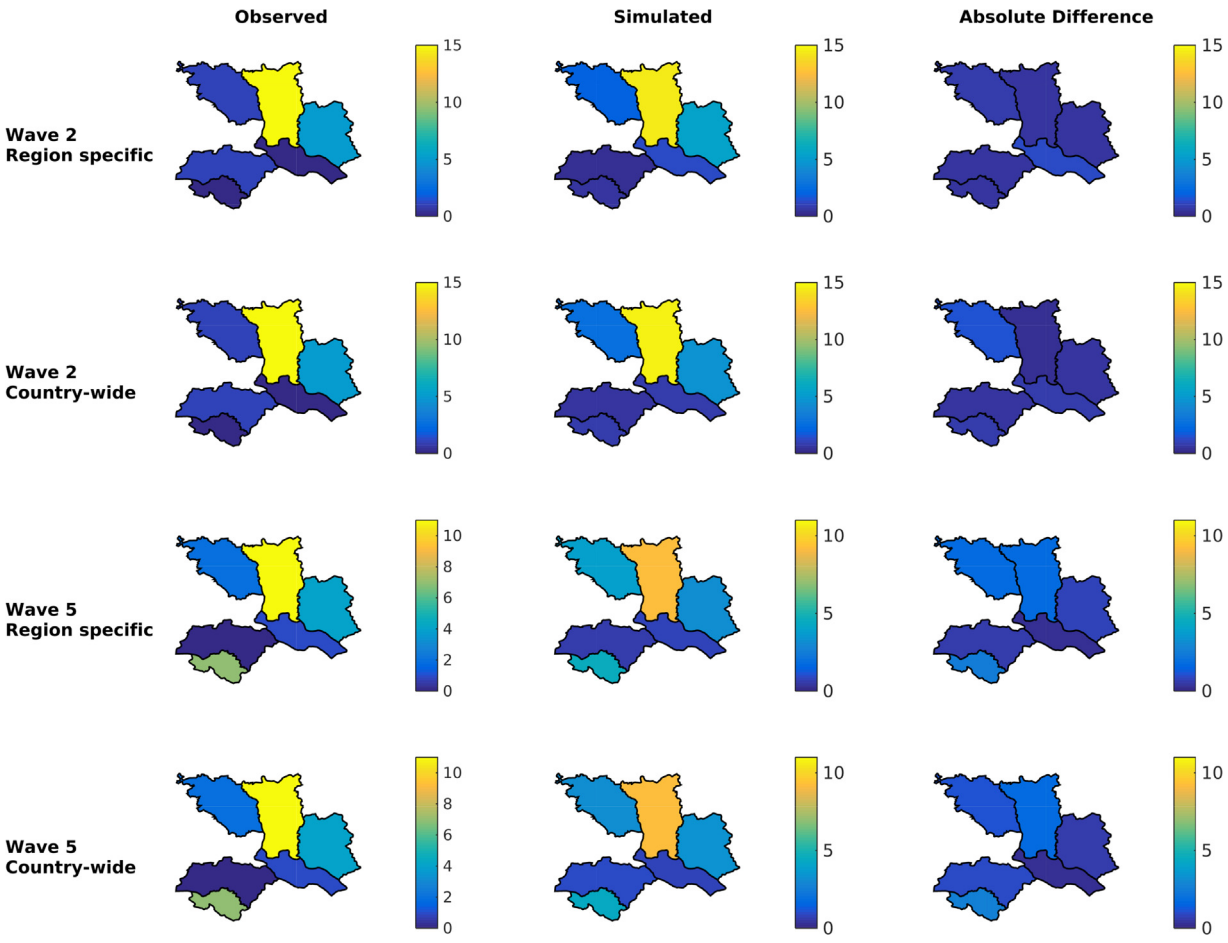

Fig. 8. Simulated infected premises numbers aggregated at the sub-district level versus observed data for all district model datasets. For each district-model dataset the first column shows the empirical data, with the second column showing the mean number of infected premises per sub-district obtained from ten simulations. The third column gives the absolute difference between these two values. In all panels lighter colours correspond to greater values. We see a reasonable spatial fit between the observed and simulated data, with the general spatial pattern captured by the model simulations. (For interpretation of the references to colour in this figure legend, the reader is referred to the web version of the article.)

hygienic measures from FAO did not seemingly impact the relative risk of H5N1 circulation in LBMs (Biswas et al., 2012). To ensure future policy recommendations are well informed, the quantitative evaluation of proposed intervention strategies to reduce the zoonotic transmission risk of influenza warrants further study. This can encompass both traditional methods (culling, vaccination, targeted surveillance) and innovative direct interruption strategies, such as intermittent government purchase plans (so that farms can be poultry-free for a short time and undergo disinfection) or restrictions on species composition (to synchronise flocks to the same birth-to-market schedule and allow for disinfection between flocks).

Inspecting the inferred parameter distributions for our division-level models revealed an apparent contrast in transmission dynamics across epidemic waves. For wave 2, the fitted transmission kernel exhibited similar values regardless of the distance between premises involved in an infection event (with $\alpha < 0$). On the other hand, the wave 5 data-informed model gave a stronger preference towards short-range transmission ($\alpha \approx 0$). Further, the force of infection was amplified by increasing the infected premises population size ($q > 1$), providing the rationale for our simulations with this fitted model determining that the regions with the greatest infection risk lay to the north of the observed cases (Supplementary Fig. S8).

These differing transmission characteristics between epidemic waves may have been the result of either a combination of, or solely, a change in disease dynamics and surveillance sensitivity. During the wave 5 poultry epidemic in 2011 a new clade of H5, 2.3.2.1, was identified in Bangladesh (Islam et al., 2012; World Health, 2014). The introduction of this virus could have altered transmission patterns compared to the viruses circulating during 2008, including how the force of infection scaled with the premises flock size. Additionally, spatial and temporal changes in surveillance between the two poultry epidemics of interest may have altered the proportion of infected cases actually reported. With the surveillance system mainly relying on passive surveillance, substantial under-reporting of poultry cases may have occurred (FAO, 2011). However, due to experiencing a number of previous epidemics by 2011 there may have been a reduction in this factor since 2008. A greater proportion of subsequent infections occurring in the local neighbourhood of an already infected premises may therefore have been found in the wave 5 epidemic of 2011, giving extra weight to short-range transmission events relative to the wave 2 fitted model.

Our preferred wave 5 division model revealed the presence of premises with "super-spreader" potential, where premises-level productive ratios R_i were much larger than one. In total, 25 premises obtained an $R_i > 10$. These had large poultry populations (at least 25,000, with only 33 premises in the entire Dhaka division having populations at or above this level) and were situated in areas with a high concentration of poultry farms. We speculate these conditions enhance the ability of a premise to transmit infection, with epidemics of greater magnitude compared to when these premises do

Please cite this article in press as: Hill, E.M., et al., Modelling H5N1 in Bangladesh across spatial scales: Model complexity and zoonotic transmission risk. Epidemics (2017), http://dx.doi.org/10.1016/j.epidem.2017.02.007

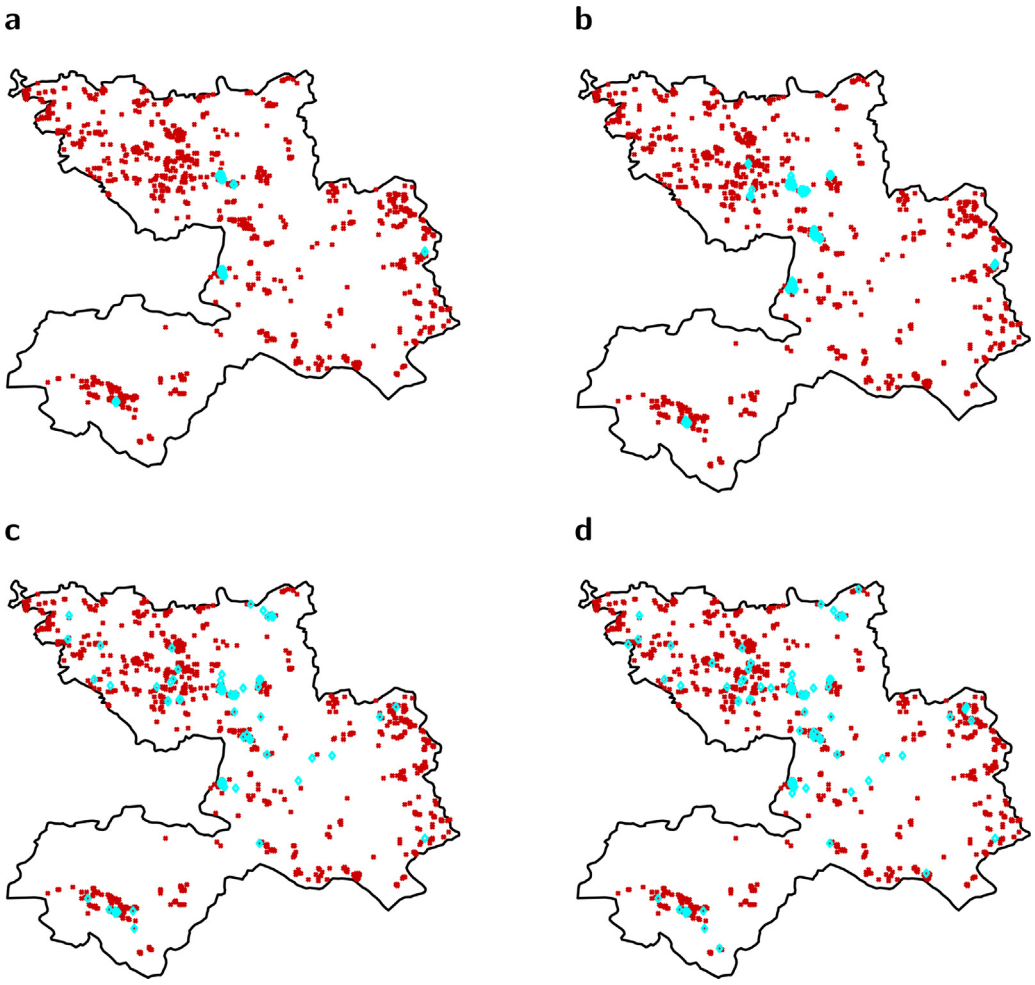

Fig. 9. Binary indicator of premises-level reproductive ratios R_i being greater than one for the district-level models. Red crosses denote premises with a $R_i < 1$, cyan diamonds premises with $R_i \geq 1$. Across the models only a limited number of premises obtained premises-level reproductive ratios greater than one. However, small clusters of premises with $R_i > 1$ were present in the centre third of the district for both waves, and in the south-west and north-west for wave 5. (a) Wave 2, region-specific epidemic dates; (b) wave 2, country-wide epidemic dates; (c) wave 5, region-specific epidemic dates; (d) wave 5, country-wide epidemic dates. (For interpretation of the references to colour in this figure legend, the reader is referred to the web version of the article.)

not become infected. A bimodal distribution for infected premises epidemic size would subsequently be expected, in agreement with our simulations (Fig. 10e). Crucially, these regions were very localised and the observed cases were predominately absent from them, with $R_i < 1$ for the majority of the division (Supplementary Fig. S9). The small scale of the wave 5 epidemic may have been a direct result of this. Such behaviour may have occurred as a result of heterogeneity in biosecurity compliance. Industrial premises with larger flock sizes implement clearly defined standard operating procedures for biosecurity (FAO, 2008). In contrast, smaller scale commercial operations may suffer from having less strict measures, such as village farms frequently being built side by side with little separation, which may promote the spread of H5N1 (The World Bank, 2013). This emphasises the importance of maintaining compliance of biosecurity regulations, preventing premises with super-spreader potential becoming infected, echoing conclusions drawn by the FAO who stated there was a strong need to improve biosecurity in commercial and government poultry farms in Bangladesh (FAO, 2008).

At the district level, premises-level reproductive ratios suggested that, in principle, chains of transmission from premises-to-premises would not be sustained. Thus, importations and transmission from other sources appeared to be vital contributors to the poultry outbreak size. Ultimately, this culminates in a low risk of infection across the entire region. This may be a consequence of the poultry value chain, with commercial poultry farms sourcing day-old chicks from a limited set of parent stock farms and grand parent farms (FAO, 2008). In other words, there is a risk of disease transfer from grand parent or parent farms to the producers, rather than via a chain of transmission occurring between-premises within the district itself. An issue to highlight is the potential for cases caused by premises that lay outside the district (so effectively imported in). While these may in fact have been a short-range transmission event from premises just outside the district, if there were infected premises in the district that were further away the fitting procedure could give a misleading level of support for long-range transmission. This leads to a further knock-on effect with the spark term value, as true infection importation events should be solely captured by that term.

The zoonotic transmission element of our modelling framework discerned differing causal mechanisms for the reported zoonotic spillover events across waves. Infected poultry is no doubt a baseline causal factor, but such event occurrences may also be influenced by LBM specific risk factors like poor biosecurity and slaughter practices (FAO, 2008). Due to wave 2 only containing a single human case there was a higher chance it was caused by the latter, with ϵ_h encapsulating such determinants. On the other hand, the human cases within wave 5 had a greater association with the

Please cite this article in press as: Hill, E.M., et al., Modelling H5N1 in Bangladesh across spatial scales: Model complexity and zoonotic transmission risk. Epidemics (2017), http://dx.doi.org/10.1016/j.epidem.2017.02.007

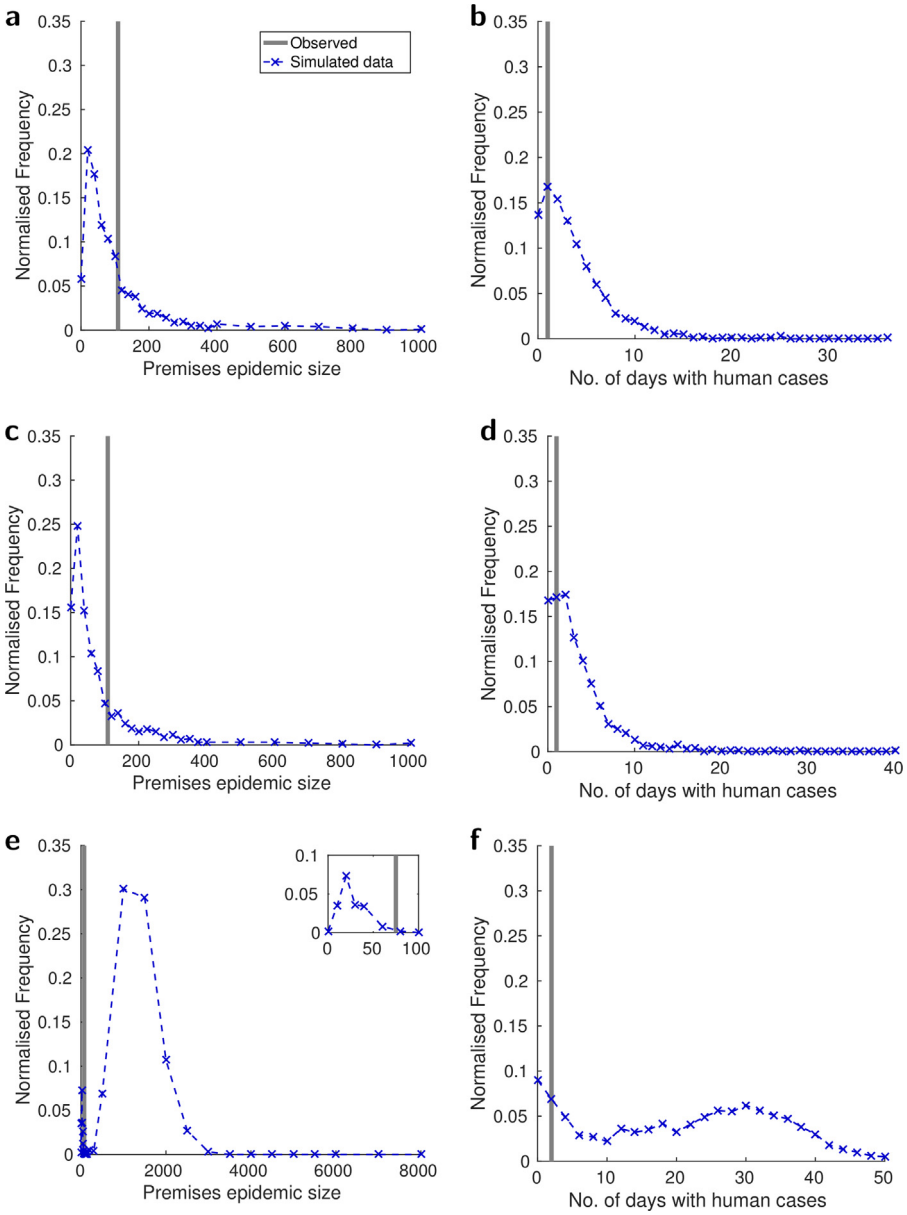

Fig. 10. Simulated epidemic size versus observed data at the division level. (a, c, e) Poultry epidemic size. (b, d, f) Human epidemic size. First row (a, b) used wave 2 region-specific epidemic dates, second row (c, d) used wave 2 country-wide epidemic dates, final row (e, f) used wave 5 epidemic dates.

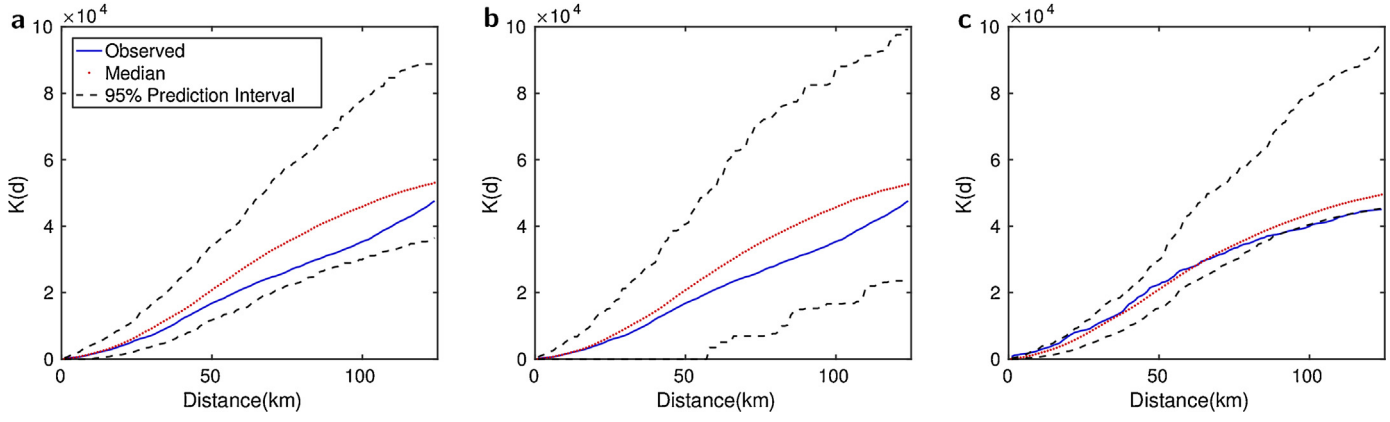

Fig. 11. Observed Ripley's K function versus simulated Ripley's K function distribution for division-level models. The Ripley's K function for the observed infected premises data is given by the solid blue line. Median Ripley's K function estimated from simulated data is represented by the red dotted line, with the black dashed lines giving the 95% prediction interval bounds. The observed data lay within the 95% prediction interval for all division-level models. (a) Wave 2, region-specific epidemic dates; (b) wave 2, country-wide epidemic dates; (c) wave 5. (For interpretation of the references to colour in this figure legend, the reader is referred to the web version of the article.)

Please cite this article in press as: Hill, E.M., et al., Modelling H5N1 in Bangladesh across spatial scales: Model complexity and zoonotic transmission risk. Epidemics (2017), http://dx.doi.org/10.1016/j.epidem.2017.02.007

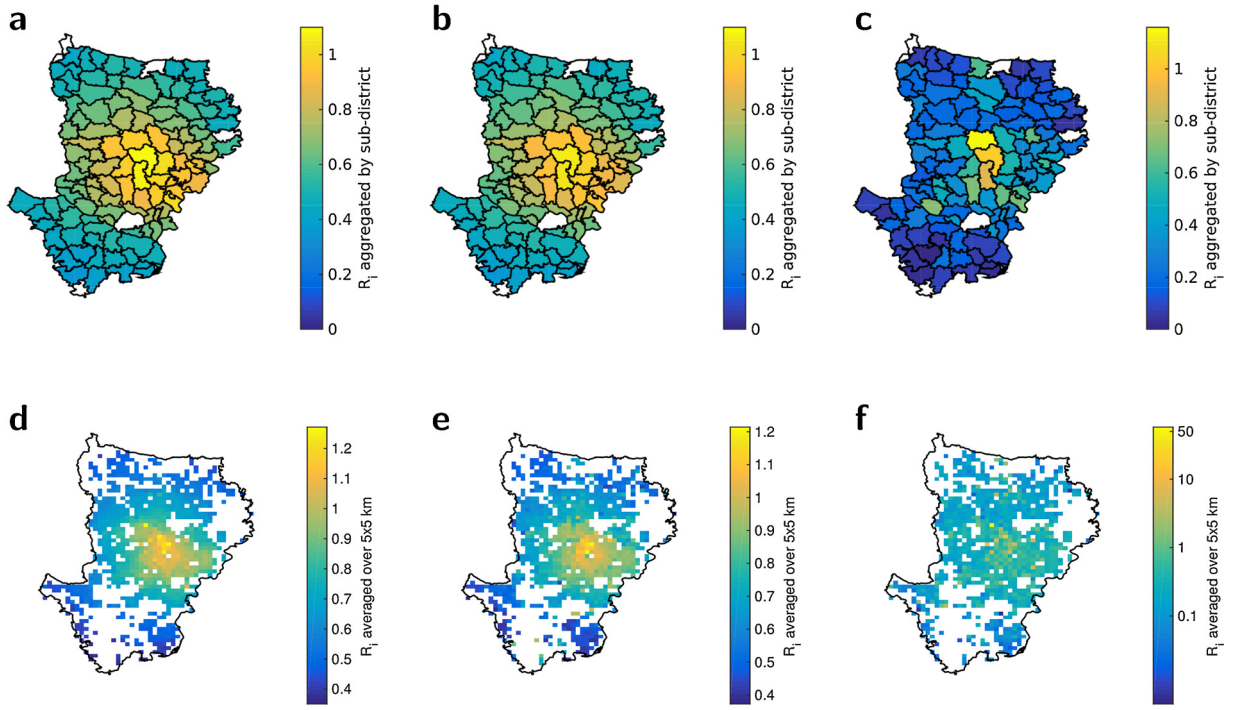

Fig. 12. Aggregated premises-level reproductive ratios R_i for the division-level models. Aggregated values were evaluated by taking the mean R_i over all individual premises situated in the region of interest, with lighter colours indicating a higher average premises-level reproductive ratio. First column used the wave 2 model fitted to region-specific epidemic dates; second column used the wave 2 model fitted to country-wide epidemic dates; final column used the wave 5 model. The highest R_i values across the two waves were in a similar area, though these were only just above one for wave 2 and smaller in scale when compared to wave 5. (a–c) R_i aggregated by sub-district; (d–f) R_i aggregated into 5 km × 5 km regions. (For interpretation of the references to colour in this figure legend, the reader is referred to the web version of the article.)

number of infected poultry, a consequence of the reduced chances of them both being caused by alternative determinants. Fitting to the wave 6 human case data, ascertaining that the ϵ_h term dominated the zoonotic transmission dynamics is in agreement with the World Health Organisation reporting LBMs as the source of infection for these specific cases (World Health Organisation, 2012).

In terms of minimising human risk, the study presented here suggests merely limiting the size of the poultry outbreak may not in isolation reduce the risk of spillover transmission, while reducing contact between humans and poultry would be prudent. Yet, we note that due to the low number of confirmed human cases we cannot attain strong evidence for these conclusions as they are supported by very few events. Furthermore, there are likely to be inherent biases in the reporting of human cases. Intensive community surveillance efforts only happen in a few communities, meaning many cases may have been missed (Nasreen et al., 2015). Additional human cases correlating temporally with peaks in poultry infection would strengthen the models preference for human case occurrence being linked to H5N1 prevalence in poultry. In light of these conditions, further study is required to verify these findings and ascertain their sensitivity to differing levels of under-reporting. Such analysis is becoming feasible through the development of novel methods for fitting models to an unknown number of infections, including fully Bayesian approaches (Jewell et al., 2009a, 2009b).

The quality of data used had some limitations. Firstly, the following inherent reporting biases could exist and have been discussed above: under-reporting can result in the true extent of both poultry and human cases not being known; the likelihood of an infected premises reporting the outbreak may increase the larger the flock size. Second, in the absence of information on the premises notification time for reporting disease we assumed all premises had the same fixed value reporting delay, treating it as an unknown parameter with a set of different plausible values tested. In reality, there is likely to be variability in this value across premises that may influence the estimated transmission parameters. Third, we chose not to include premises locations that had no poultry populations present in the poultry census database. While this should portray the proportion of premises that are between-flocks at any one time, the impact of alternative sets of poultry farms being populated at a given moment, with the effect on risk of zoonotic H5N1 transmission that follows, requires further study. Further, our assumption of culled premises not being restocked while a poultry epidemic was still in progress may not hold for all our datasets, as in reality the restocking period following a cull is three months (World Organisation for Animal Health, 2015). Fourth, due to not having data on movements of poultry we were unable to include highly preferential trading links between premises and LBMs explicitly in our analysis. However, previous work concluded that when proposing models for animal movement contact data between holdings, those that included separate distance-dependent and distance-independent terms were preferred to purely distance dependent models (Lindström et al., 2009). This therefore motivated our model framework including both a fitted distance-dependent transmission kernel and a spark term to seed infections from other sources independent of distance. Finally, factors that have been previously determined to increase risk of H5N1 infection in poultry, such as the number of roads per sub-district and human population density (Loth et al., 2010), were not incorporated here. Further work focused specifically on these factors should be able to enhance understanding of public accessibility as a H5N1 poultry infection risk.

To address this the modelling framework outlined can be extended in numerous ways. The first would be to treat layer and broiler chickens as distinct types, rather than considering the total poultry population per premises. It could then be ascertained whether there are type-specific risk factors or, for a specific risk factor, differing levels of risk against each poultry type.

Please cite this article in press as: Hill, E.M., et al., Modelling H5N1 in Bangladesh across spatial scales: Model complexity and zoonotic transmission risk. Epidemics (2017), http://dx.doi.org/10.1016/j.epidem.2017.02.007

Next, as previously discussed, while we have focused on a linear dependence on the presence/absence of a number of covariates and the resulting contribution to overall risk of infection, many other choices for the spark term dependence could be made. For example, if the necessary data were available, a non-distance dependency on LBMs could be used based on total LBM visits from personnel working on the premises of interest. The impact of varying these dependencies merits further investigation. Thirdly, restocking of previously culled premises can be integrated into the poultry transmission model component, while modifications can be made to the zoonotic transmission component to produce a complete spatially dependent model. Implementing these changes would allow information such as human population density and LBM locations to be explicitly incorporated. Another direction for further work is to relax the assumption of every premises having the same delay-time for reporting disease, and to determine the robustness of the modelling framework by applying it to other regions that have recorded H5N1 cases in both poultry and humans.

Overall, with the data available, our findings suggest the key components that should be incorporated within a general division-level framework for H5N1 poultry infection in Bangladesh were identifiable (despite apparent differences in behaviour for each poultry epidemic of interest), while this was not achievable at the district administration level. Across spatial scales we saw a consistent outcome of non-optimal reporting of infected premises, suggesting we should seek procedural improvements that will reduce the notification time of infected poultry premises. Furthermore, our simple zoonotic transmission model capably identified differing significant contributors to spillover transmission from poultry to humans across epidemics. Yet, for H5N1 influenza the dynamic interplay between animal health, environmental factors and the immune system of the human host must be resolved to ensure policy decisions result in the minimisation of zoonotic transmission occurrence. Given these complexities, it is imperative that further work to enhance understanding of influenza transmission dynamics at the human–animal interface is pursued.

Author contributions

M.J.T, E.M.H, M.G. and T.H. planned the study. W.K., S.M., M.G.O, X.X. and M.Y. contributed data. E.M.H. performed the model fitting and simulations. E.M.H., T.H., M.S.D, M.G. and M.J.T. analysed the results. E.M.H., T.H., M.S.D, W.K., S.M., M.G.O, X.X., M.Y., M.G. and M.J.T. contributed to the writing of the manuscript. All authors gave final approval for publication.

Financial disclosure

EMH, MJT and TH are supported by the Engineering and Physical Sciences Research Council [grant numbers EP/I01358X/1, EP/P511079/1, EP/N033701/1]. MD, XX, MG and MJT are supported by the National Institutes of Health (NIH grant number 1R01AI101028-01A1). MJT is supported by the RAPIDD program of the Science and Technology Directorate, Department of Homeland Security, and the Fogarty International Center, National Institutes of Health. The work described in this paper was partially supported by the United States Agency for International Development Emerging Pandemic Threats Programme and the grant from the United States Agency for International Development SRO/BGD/303/USA: Strengthening National Capacity to Respond to Highly Pathogenic Avian Influenza (HPAI) and Emerging and Re-Emerging Diseases in Bangladesh. The work utilised Queen Mary's Midplus computational facilities supported by QMUL Research-IT and funded by Engineering and Physical Sciences Research Council grant EP/K000128/1. The funders had no role in study design, data collection and analysis, decision to publish, or preparation of the manuscript.

Acknowledgements

We thank the Bangladesh Department of Livestock Services (DLS) for providing the premises and live bird market data. Colleagues at FAO-ECTAD (Emergency Centre for Transboundary Animal Diseases) office in Bangladesh are thanked for their contribution. The work described in the paper was partially supported by the USAID Emerging Pandemic Threats Programme (EPT) and the authors would like to thank them for their continued support.

Appendix A. Supplementary data

Supplementary data associated with this article can be found, in the online version, at http://dx.doi.org/10.1016/j.epidem.2017.02.007.

References

Ahmed, S.S.U., Ersbøll, A.K., Biswas, P.K., Christensen, J.P., 2010. The spacetime clustering of highly pathogenic avian influenza (HPAI) H5N1 outbreaks in Bangladesh. Epidemiol. Infect. 138 (06), 843, http://dx.doi.org/10.1017/S0950268810000178.

Ahmed, S.S.U., Ersbøll, A.K., Biswas, P.K., Christensen, J.P., Toft, N., 2011. Spatio-temporal magnitude and direction of highly pathogenic avian influenza (H5N1) outbreaks in Bangladesh. PLoS ONE 6 (9), e24324, http://dx.doi.org/10.1371/journal.pone.0024324.

Ahmed, S.S.U., Ersbøll, A.K., Biswas, P.K., Christensen, J.P., Hannan, A.S.M.A., Toft, N., 2012. Ecological determinants of highly pathogenic avian influenza (H5N1) outbreaks in Bangladesh. PLoS ONE 7 (3), e33938, http://dx.doi.org/10.1371/journal.pone.0033938.

Alexander, D.J., 2007. Summary of avian influenza activity in Europe, Asia, Africa, and Australasia, 2002–2006. Avian Dis. 51 (s1), 161–166, http://dx.doi.org/10.1637/7602-041306R.1.

Ansari, W.K., Parvej, M.S., El Zowalaty, M.E., Jackson, S., Bustin, S.A., Ibrahim, A.K., El Zowalaty, A.E., Rahman, M.T., Zhang, H., Khan, M.F.R., Ahamed, M.M., Rahman, M.F., Rahman, M., Nazir, K.N.H., Ahmed, S., Hossen, M.L., Kafi, M.A., Yamage, M., Debnath, N.C., Ahmed, G., Ashour, H.M., Masudur Rahman, M., Noreddin, A., Rahman, M.B., 2016. Surveillance, epidemiological, and virological detection of highly pathogenic H5N1 avian influenza viruses in duck and poultry from Bangladesh. Vet. Microbiol. 193, 49–59, http://dx.doi.org/10.1016/j.vetmic.2016.07.025.

Arino, O., Perez, J.J.R., Kalogirou, V., Bontemps, S., Defourny, P., Van Bogaert, E., 2012, August. Global Land Cover Map for 2009 (GlobCover 2009)., http://dx.doi.org/10.1594/PANGAEA.787668.

Biswas, P.K., Christensen, J.P., Ahmed, S.S.U., Barua, H., Das, A., Rahman, M.H., Giasuddin, M., Hannan, A.S.M.A., Habib, A.M., Debnath, N.C., 2009a. Risk factors for infection with highly pathogenic influenza A virus (H5N1) in commercial chickens in Bangladesh. Vet. Rec. 164 (24), 743–746, http://dx.doi.org/10.1136/vr.164.24.743.

Biswas, P.K., Christensen, J.P., Ahmed, S.S., Das, A., Rahman, M.H., Barua, H., Giasuddin, M., Hannan, A.S., Habib, M.A., Debnath, N.C., 2009b. Risk for infection with highly pathogenic avian influenza virus (H5N1) in backyard chickens, Bangladesh. Emerg. Infect. Dis. 15 (12), 1931–1936, http://dx.doi.org/10.3201/eid1512.090643.

Biswas, P.K., Christensen, J.P., Ahmed, S.S.U., Barua, H., Das, A., Rahman, M.H., Giasuddin, M., Habib, M.A., Hannan, A.S.M.A., Debnath, N.C., 2011. Mortality rate and clinical features of highly pathogenic avian influenza in naturally infected chickens in Bangladesh. Rev. Sci. Tech. 30 (3), 871–878.

Biswas, P.K., Giasuddin, M., Nath, B.K., Islam, M.Z., Debnath, N.C., Yamage, M., 2015. Biosecurity and circulation of influenza A (H5N1) virus in live-bird markets in Bangladesh, 2012. Transbound. Emerg. Dis., http://dx.doi.org/10.1111/tbed.12454.

Bouma, A., Claassen, I., Natih, K., Klinkenberg, D., Donnelly, C.A., Koch, G., van Boven, M., 2009. Estimation of transmission parameters of H5N1 avian influenza virus in chickens. PLoS Pathog. 5 (1), e1000281, http://dx.doi.org/10.1371/journal.ppat.1000281.

Deardon, R., Brooks, S.P., Grenfell, B.T., Keeling, M.J., Tildesley, M.J., Savill, N.J., Shaw, D.J., Woolhouse, M.E.J., 2010. Inference for individual-level models of infectious diseases in large populations. Stat. Sin. 20 (1), 239–261.

Dejpichai, R., Laosiritaworn, Y., Phuthavathana, P., Uyeki, T.M., O'Reilly, M., Yampikulsakul, N., Phurahong, S., Poorak, P., Prasertsopon, J., Kularb, R., Nateerom, K., Sawanpanyalert, N., Jiraphongsa, C., 2009. Seroprevalence of antibodies to avian influenza virus A (H5N1) among residents of villages with human cases, Thailand, 2005. Emerg. Infect. Dis. 15 (5), 756–760, http://dx.doi.org/10.3201/eid1505.080316.

Dhingra, M.S., Dissanayake, R., Negi, A.B., Oberoi, M., Castellan, D., Thrusfield, M., Linard, C., Gilbert, M., 2014. Spatio-temporal epidemiology of highly pathogenic avian influenza (subtype H5N1) in poultry in eastern India. Spat. Spatiotemporal Epidemiol. 11, 45–57, http://dx.doi.org/10.1016/j.sste.2014.06.003.

FAO, 2008. Poultry Sector Country Review Bangladesh.

FAO, Approaches to controlling, preventing and eliminating H5N1 Highly Pathogenic Avian Influenza in endemic countries, *Anim. Prod. Heal. Pap.* (No. 171), 2011.

FAO, EMPRES-i. http://empres-i.fao.org/eipws3g/.

FAO-DAH, 2012. H5N1 HPAI Global Overview: April–June 2012. http://www.fao.org/docrep/016/ap387e/ap387e.pdf.

Farnsworth, M.L., Hamilton-West, C., Fitchett, S., Newman, S.H., de La Rocque, S., De Simone, L., Lubroth, J., Pinto, J., 2010. Comparing national and global data collection systems for reporting, outbreaks of H5N1 HPAI. Prev. Vet. Med. 95 (3–4), 175–185, http://dx.doi.org/10.1016/j.prevetmed.2010.03.012.

Gelman, A., Carlin, J., Stern, H., Rubin, D., 2003. Bayesian Data Analysis, 2nd ed. Chapman and Hall/CRC.

Gilbert, M., Pfeiffer, D.U., 2012. Risk factor modelling of the spatio-temporal patterns of highly pathogenic avian influenza (HPAIV) H5N1: a review. Spat. Spatiotemporal Epidemiol. 3 (3), 173–183, http://dx.doi.org/10.1016/j.sste.2012.01.002.

Gilbert, M., Xiao, X., Chaitaweesub, P., Kalpravidh, W., Premashthira, S., Boles, S., Slingenbergh, J., 2007. Avian influenza, domestic ducks and rice agriculture in Thailand. Agric. Ecosyst. Environ. 119 (3-4), 409–415, http://dx.doi.org/10.1016/j.agee.2006.09.001.

Gilbert, M., Xiao, X., Pfeiffer, D.U., Epprecht, M., Boles, S., Czarnecki, C., Chaitaweesub, P., Kalpravidh, W., Minh, P.Q., Otte, M.J., Martin, V., Slingenbergh, J., 2008. Mapping H5N1 highly pathogenic avian influenza risk in Southeast Asia. Proc. Natl. Acad. Sci. U. S. A. 105 (12), 4769–4774, http://dx.doi.org/10.1073/pnas.0710581105.

Gilbert, M., Newman, S.H., Takekawa, J.Y., Loth, L., Biradar, C., Prosser, D.J., Balachandran, S., Subba Rao, M.V., Mundkur, T., Yan, B., Xing, Z., Hou, Y., Batbayar, N., Natsagdorj, T., Hogerwerf, L., Slingenbergh, J., Xiao, X., 2010. Flying over an infected landscape: distribution of highly pathogenic avian influenza H5N1 risk in south Asia and satellite tracking of wild waterfowl. Ecohealth 7 (4), 448–458, http://dx.doi.org/10.1007/s10393-010-0672-8.

Gillespie, D.T., 2001. Approximate accelerated stochastic simulation of chemically reacting systems. J. Chem. Phys. 115 (4), 1716–1733, http://dx.doi.org/10.1063/1.1378322.

Haario, H., Saksman, E., Tamminen, J., 2001. An adaptive Metropolis algorithm. Bernoulli 7 (2), 223–242.

Hancock, P.A., Rehman, Y., Hall, I.M., Edeghere, O., Danon, L., House, T.A., Keeling, M.J., 2014. Strategies for controlling non-transmissible infection outbreaks using a large human movement data set. PLoS Comput. Biol. 10 (9), e1003809, http://dx.doi.org/10.1371/journal.pcbi.1003809.

Henning, K.A., Henning, J., Morton, J., Long, N.T., Ha, N.T., Meers, J., 2009. Farm- and flock-level risk factors associated with highly pathogenic avian influenza outbreaks on small holder duck and chicken farms in the Mekong Delta of Viet Nam. Prev. Vet. Med. 91 (2–4), 179–188, http://dx.doi.org/10.1016/j.prevetmed.2009.05.027.

Islam, M.R., Haque, M.E., Giasuddin, M., Chowdhury, E.H., Samad, M.A., Parvin, R., Nooruzzaman, M., Rahman, M.M., Monoura, P., 2012. New introduction of clade 2.3.2.1 avian influenza virus (H5N1) into Bangladesh. Transbound. Emerg. Dis. 59 (5), 460–463, http://dx.doi.org/10.1111/j.1865-1682.2011.01297.x.

Jewell, C.P., Kypraios, T., Neal, P., Roberts, G.O., 2009a. Bayesian analysis for emerging infectious diseases. Bayesian Anal. 4 (3), 465–496, http://dx.doi.org/10.1214/09-BA417.

Jewell, C., Kypraios, T., Christley, R., Roberts, G., 2009b. A novel approach to real-time risk prediction for emerging infectious diseases: a case study in avian influenza H5N1. Prev. Vet. Med. 91 (1), 19–28, http://dx.doi.org/10.1016/j.prevetmed.2009.05.019.

Keeling, M., Rohani, P., 2008. Modeling Infectious Diseases in Humans and Animals. Princeton University Press.

Keeling, M.J., Woolhouse, M.E., Shaw, D.J., Matthews, L., Chase-Topping, M., Haydon, D.T., Cornell, S.J., Kappey, J., Wilesmith, J., Grenfell, B.T., 2001. Dynamics of the 2001 UK foot and mouth epidemic: stochastic dispersal in a heterogeneous landscape. Science 294 (5543), 813–817, http://dx.doi.org/10.1126/science.1065973.

Lindström, T., Sisson, S.A., Nöremark, M., Jonsson, A., Wennergren, U., 2009. Estimation of distance related probability of animal movements between holdings and implications for disease spread modeling. Prev. Vet. Med. 91 (2–4), 85–94, http://dx.doi.org/10.1016/j.prevetmed.2009.05.022.

Lloyd-Smith, J.O., George, D., Pepin, K.M., Pitzer, V.E., Pulliam, J.R.C., Dobson, A.P., Hudson, P.J., Grenfell, B.T., 2009. Epidemic dynamics at the human–animal interface. Science 326 (5958), 1362–1367, http://dx.doi.org/10.1126/science.1177345.

Lloyd-Smith, J.O., Funk, S., McLean, A.R., Riley, S., Wood, J.L., 2015. Nine challenges in modelling the emergence of novel pathogens. Epidemics 10, 35–39, http://dx.doi.org/10.1016/j.epidem.2014.09.002.

Loth, L., Gilbert, M., Osmani, M.G., Kalam, A.M., Xiao, X., 2010. Risk factors and clusters of highly pathogenic avian influenza H5N1 outbreaks in Bangladesh. Prev. Vet. Med. 96 (1–2), 104–113, http://dx.doi.org/10.1016/j.prevetmed.2010.05.013.

Minh, P.Q., Stevenson, M.A., Jewell, C., French, N., Schauer, B., 2011. Spatio-temporal analyses of highly pathogenic avian influenza H5N1 outbreaks in the Mekong River Delta, Vietnam, 2009. Spat. Spatiotemporal Epidemiol. 2 (1), 49–57, http://dx.doi.org/10.1016/j.sste.2010.11.001.

Nasreen, S., Khan, S.U., Luby, S.P., Gurley, E.S., Abedin, J., Zaman, R.U., Sohel, B.M., Rahman, M., Hancock, K., Levine, M.Z., Veguilla, V., Wang, D., Holiday, C., Gillis, E., Sturm-Ramirez, K., Bresee, J.S., Rahman, M., Uyeki, T.M., Katz, J.M., Azziz-Baumgartner, E., 2015. Highly pathogenic avian influenza A (H5N1) virus infection among workers at live bird markets, Bangladesh, 2009–2010. Emerg. Infect. Dis. 21 (4), 629–637, http://dx.doi.org/10.3201/eid2104.141281.

Neal, R.M., 2003. Slice sampling. Ann. Stat. 31 (3), 705–767, http://dx.doi.org/10.1214/aos/1056562461.

OIE, 2013. Highly pathogenic avian influenza, Bangladesh (Follow-up report No. 43), OIE, WAHID (World Anim. Heal. Inf. Database). Wkly Dis. Inf. 26 (52).

Osmani, M.G., Thornton, R.N., Dhand, N.K., Hoque, M.A., Milon, S.M.A., Kalam, M.A., Hossain, M., Yamage, M., 2014a. Risk factors for highly pathogenic avian influenza in commercial layer chicken farms in Bangladesh during 2011. Transbound. Emerg. Dis. 61 (6), e44–e51, http://dx.doi.org/10.1111/tbed.12071.

Osmani, M.G., Ward, M.P., Giasuddin, M., Islam, M.R., Kalam, A., 2014b. The spread of highly pathogenic avian influenza (subtype H5N1) clades in Bangladesh, 2010 and 2011. Prev. Vet. Med. 114 (1), 21–27, http://dx.doi.org/10.1016/j.prevetmed.2014.01.010.

Pfeiffer, D.U., Minh, P.Q., Martin, V., Epprecht, M., Otte, M.J., 2007. An analysis of the spatial and temporal patterns of highly pathogenic avian influenza occurrence in Vietnam using national surveillance data. Vet. J. 174 (2), 302–309, http://dx.doi.org/10.1016/j.tvjl.2007.05.010.

Rabinowitz, P.M., Galusha, D., Vegso, S., Michalove, J., Rinne, S., Scotch, M., Kane, M., 2012. Comparison of human and animal surveillance data for H5N1 influenza A in Egypt 2006–2011. PLoS ONE 7 (9), e43851, http://dx.doi.org/10.1371/journal.pone.0043851.

Ripley, B.D., 1976. The second-order analysis of stationary point processes. J. Appl. Probab. 13 (2), 255–266, http://dx.doi.org/10.2307/3212829.

Ripley, B.D., 1977. Modelling spatial patterns. J. R. Stat. Soc. Ser. B 39 (2), 172–212.

Robinson, T., Wint, G., Conchedda, G., Van Boeckel, T., Ercoli, V., Palamara, E., Cinardi, G., D'Aietti, L., Hay, S., Gilbert, M., 2014. Mapping the global distribution of livestock. PLOS ONE 9 (5), e96084, http://dx.doi.org/10.1371/journal.pone.0096084.

Sims, L.D., Domenech, J., Benigno, C., Kahn, S., Kamata, A., Lubroth, J., Martin, V., Roeder, P., 2005. Origin and evolution of highly pathogenic H5N1 avian influenza in Asia. Vet. Rec. 157 (6), 159–164, http://dx.doi.org/10.1136/vr.157.6.159.

Spiegelhalter, D.J., Best, N.G., Carlin, B.P., van der Linde, A., 2002. Bayesian measures of model complexity and fit. J. R. Stat. Soc. Ser. B (Stat. Methodol. 64 (4), 583–639, http://dx.doi.org/10.1111/1467-9868.00353.

The World Bank, 2013. Implementation completion and results report (IDA-43400 TF-90662) on a credit in the amount of SDR 10.5 million (US $ 16.0 million equivalent) to the People's Republic of Bangladesh for an avian influenza preparedness and response project under the global. http://documents.worldbank.org/curated/en/651381468210870082/pdf/ICR21770ICR0Av0Box0377341B00PUBLIC0.pdf.

Tiensin, T., Nielen, M., Vernooij, H., Songserm, T., Kalpravidh, W., Chotiprasatintara, S., Chaisingh, A., Wongkasemjit, S., Chanachai, K., Thanapongtham, W., Srisuvan, T., Stegeman, A., 2007. Transmission of the highly pathogenic avian influenza virus H5N1 within flocks during the 2004 epidemic in Thailand. J. Infect. Dis. 196 (11), 1679–1684, http://dx.doi.org/10.1086/522007.

Tildesley, M.J., Keeling, M.J., 2009. Is R_0 a good predictor of final epidemic size: foot-and-mouth disease in the UK. J. Theor. Biol. 258 (4), 623–629, http://dx.doi.org/10.1016/j.jtbi.2009.02.019.

Tildesley, M.J., Deardon, R., Savill, N.J., Bessell, P.R., Brooks, S.P., Woolhouse, M.E.J., Grenfell, B.T., Keeling, M.J., 2008. Accuracy of models for the 2001 foot-and-mouth epidemic. Proc. R. Soc. London B: Biol. Sci. 275 (1641), 1459–1468, http://dx.doi.org/10.1098/rspb.2008.0006.

United Nations, 2015. Department of Economic and Social Affairs: Population Division, World Population Prospects, the 2015 Revision. http://www.un.org/en/development/desa/population/theme/trends/index.shtml.

Van Boeckel, T.P., Thanapongtharm, W., Robinson, T., Biradar, C.M., Xiao, X., Gilbert, M., 2012. Improving risk models for avian influenza: the role of intensive poultry farming and flooded land during the 2004 Thailand epidemic. PLoS ONE 7 (11), e49528, http://dx.doi.org/10.1371/journal.pone.0049528.

World Health Organisation, 2012. Influenza at the Human-Animal Interface: Summary and assessment as of 5 March 2012. http://www.who.int/influenza/human_animal_interface/Influenza_Summary_IRA_HA_interface_05March12.pdf?ua=1.

World Health Organisation, 2016. Cumulative number of confirmed human cases of avian influenza A(H5N1) reported to WHO: 21 November 2016. http://www.who.int/influenza/human_animal_interface/2016_11_21_tableH5N1.pdf.

World Health Organization/World Organisation for Animal Health/Food and Agriculture Organization (WHO/OIE/FAO) H5N1 Evolution Working Group, 2014. Revised and updated nomenclature for highly pathogenic avian influenza A (H5N1) viruses. Influenza Other Respir. Viruses 8 (3), 384–388, http://dx.doi.org/10.1111/irv.12230.

World Organisation for Animal Health (OIE), 2015. Terrestrial Animal Health Code, 24th ed. OIE, Paris http://www.oie.int/international-standard-setting/terrestrial-code/access-online/.

Xiao, X., Boles, S., Liu, J., Zhuang, D., Frolking, S., Li, C., Salas, W., Moore, B., 2005. Mapping paddy rice agriculture in southern China using multi-temporal

Please cite this article in press as: Hill, E.M., et al., Modelling H5N1 in Bangladesh across spatial scales: Model complexity and zoonotic transmission risk. Epidemics (2017), http://dx.doi.org/10.1016/j.epidem.2017.02.007

MODIS images. Remote Sens. Environ. 95 (4), 480–492, http://dx.doi.org/10.1016/j.rse.2004.12.009.
Xiao, X., Boles, S., Frolking, S., Li, C., Babu, J.Y., Salas, W., Moore, B., 2006. Mapping paddy rice agriculture in South and Southeast Asia using multi-temporal MODIS images. Remote Sens. Environ. 100 (1), 95–113, http://dx.doi.org/10.1016/j.rse.2005.10.004.
Zhang, G., Xiao, X., Dong, J., Kou, W., Jin, C., Qin, Y., Zhou, Y., Wang, J., Menarguez, M.A., Biradar, C., 2015. Mapping paddy rice planting areas through time series analysis of MODIS land surface temperature and vegetation index data. ISPRS J. Photogramm. Remote Sens. 106, 157–171, http://dx.doi.org/10.1016/j.isprsjprs.2015.05.011.

Please cite this article in press as: Hill, E.M., et al., Modelling H5N1 in Bangladesh across spatial scales: Model complexity and zoonotic transmission risk. Epidemics (2017), http://dx.doi.org/10.1016/j.epidem.2017.02.007